Journal of Pharmaceutical Analysis 14 (2024) 100968

Contents lists available at ScienceDirect

Journal of Pharmaceutical Analysis

journal homepage: www.elsevier.com/locate/jpa

Original article

Baicalein: A potential GLP-1R agonist improves cognitive disorder of diabetes through mitophagy enhancement

Na Liu [a], Xin Cui [a], Wenhui Yan [a], Tingli Guo [a], Zhuanzhuan Wang [a], Xiaotong Wei [a], Yuzhuo Sun [a], Jieyun Liu [a], Cheng Xian [c], Weina Ma [b, **], Lina Chen [a, d, e, *]

[a] Department of Pharmacology, School of Basic Medical Sciences, Xi'an Jiaotong University, Xi'an, 710061, China
[b] School of Pharmacy, Xi'an Jiaotong University Health Science Center, Xi'an, 710061, China
[c] Hezhou People's Hospital, Guangxi Zhuang Autonomous Region, Hezhou, Guangxi, 542899, China
[d] Key Laboratory of Environment and Genes Related to Diseases (Xi'an Jiaotong University), Ministry of Education, Xi'an, 710061, China
[e] Cardiometabolic Innovation Center, Ministry of Education, Xi'an, 710061, China

A R T I C L E I N F O

Article history:
Received 18 October 2023
Received in revised form
22 February 2024
Accepted 20 March 2024
Available online 24 March 2024

Keywords:
GLP-1R agonist
Diabetes
Cognitive disorder
Mitophagy
Cell membrane chromatography

A B S T R A C T

There is increasing evidence that the activation of glucagon-like peptide-1 receptor (GLP-1R) can be used as a therapeutic intervention for cognitive disorders. Here, we have screened GLP-1R targeted compounds from *Scutellaria baicalensis*, which revealed baicalein is a potential GLP-1R small-molecule agonist. Mitophagy, a selective autophagy pathway for mitochondrial quality control, plays a neuroprotective role in multiple cognitive impairment diseases. We noticed that *Glp1r* knock-out (KO) mice present cognitive impairment symptoms and appear worse in spatial learning memory and learning capacity in Morris water maze (MWM) test than their wide-type (WT) counterparts. Our mechanistic studies revealed that mitophagy is impaired in hippocampus tissue of diabetic mice and *Glp1r* KO mice. Finally, we verified that the cognitive improvement effects of baicalein on diabetic cognitive dysfunction occur through the enhancement of mitophagy in a GLP-1R-dependent manner. Our findings shed light on the importance of GLP-1R for cognitive function maintenance, and revealed the vital significance of GLP-1R for maintaining mitochondrial homeostasis. Furthermore, we identified the therapeutic potential of baicalein in the treatment of cognitive disorder associated with diabetes.

1. Introduction

Type 2 diabetes mellitus (T2DM) is a severe metabolic syndrome and a public threat to human health [1]. Cognitive disorder is a common complication and comorbidity of T2DM, reflected on individuals with diabetes are more than twice likely than those without diabetes to develop cognitive decline [2,3]. Mitochondria are the center for energy production having developed rigorous mechanisms for quality control, including the regulation of mitochondrial biogenesis and the clearance of damaged components [4]. These processes synergistically facilitate the turnover of mitochondria [5]. The dysfunction of neuronal mitochondria is a prime pathological characteristic for cognitive disorder, exhibited in damaged mitochondria have been observed in brains of multiple diabetic cognitive disorder animal models [6–8]. The accumulation of dysfunctional mitochondria and following oxidative stress are main inducements for neuronal impairment [9]. Peroxisome proliferator-activated receptor-γ coactivator (PGC)-1α is a mitochondrial biogenesis regulator, and whose expression reduction contributes to synaptic dysfunction and neuronal deterioration in neurodegenerative disorders [10]. Furthermore, mitochondrial dynamics imbalance like the disorder between mitochondrial fission and fusion can also lead to neurodegenerative diseases, such as the disturbance of dynamin-related protein 1 (DRP-1) and mitofusin-2 (MFN-2) [11].

Mitophagy charactered by double-membrane autophagosomes engulf injured or depolarized mitochondria and following fuse with lysosomes for degradation, is a selective autophagy pathway for mitochondrial quality control [12]. Emerging findings suggest that compromised mitophagy along with accumulated dysfunctional mitochondria in diabetic rats contribute to neuronal apoptosis in hippocampus and cognitive decline [8]. Conversely, DA4-JC, a glucagon-like peptide-1 (GLP-1)/glucose-dependent insulinotropic polypeptide (GIP) dual receptor agonist, upregulates protein levels

* Corresponding author. Department of Pharmacology, School of Basic Medical Sciences, Xi'an Jiaotong University, Xi'an, 710061, China.
** Corresponding author.
E-mail addresses: maweina2015@mail.xjtu.edu.cn (W. Ma), chenlin@mail.xjtu.edu.cn (L. Chen).

https://doi.org/10.1016/j.jpha.2024.100968
2095-1779/

of post-synaptic density protein 95 (PSD 95) and synaptophysin (SYP), downregulates expression of amyloids and p-tau, and ameliorates memory impairment in transgenic mouse models of Alzheimer's disease (AD) through mitophagy enhancement [13].

The activation of glucagon-like peptide-1 receptor (GLP-1R) has been proved to improve memory deficit in multiple diseases, including bipolar disorder [14], diabetes-associated depression and cognitive disorder [15] and sepsis-induced encephalopathy [16]. Currently approved GLP-1R agonists (GLP-1RAs) are peptide based, notwithstanding required to be administrated by subcutaneous (s.c.) injection, having brought improved treatment outcomes for diabetic patients [17]. Semaglutide in conjunction with sodium *N*-(8-[2-hydroxybenzoyl] amino) caprylate (an absorption enhancer for oral delivery) coming into the market is a significant advance in GLP-1 therapy, although its oral bioavailability is less than 1% [18]. These elevated the importance of seeking oral small-molecule activators of GLP-1R to even greater importance. The further researches revealed that non-peptide ligands, for example 4-(3-(Benzyloxy)phenyl)-2-(ethylsulfinyl)-6-(trifluoromethyl)pyrimidine (BETP) [19], compound 2 and B [20] and LY3502970 [17] can activate GLP-1R and perform the similar effects like GLP-1 analogues.

Cell membrane chromatography (CMC) is a biomimetic chromatographic method based on the capacity of membrane receptors to selectively bond with their ligands *in vivo*, which has been wide applied to investigate the drug-receptor interactions and to screen effective components from complex samples [21]. *Scutellaria baicalensis*, a traditional Chinese herbal medicine, has shown evident effects on antioxidant [22], antidiabetic [23], antidotes [24] and neuroprotection [25]. Herein, we used CMC to screen and identify GLP-1R small-molecule agonists from *Scutellaria baicalensis*, and further confirmed baicalein (5,6,7-Trihydroxy-2-phenyl-4H-1-benzopyran-4-one, BAC) is a potential GLP-1R agonist. Our mechanism investigation verified that baicalein improves the diabetic cognitive disorder by enhancing mitophagy in a GLP-1R-dependent way.

2. Material and methods

2.1. Regents and materials

Scutellaria baicalensis was acquired from Chongqing University Fuling Hospital (Chongqing, China). BETP (≥99%) and GLP-1(7−36) (≥99%) were purchased from MedChemExpress Compound Library (Princeton, NJ, USA). Baicalein was purchased from Chengdu Pufei De Biotect. Co., Ltd. (Chengdu, China). Spherical silica gel (ZEX-II, 5 μm, 200 Å) was acquired from Qingdao Makall Group (Qingdao, China). The fetal bovine serum (FBS), Dulbecco's modified Eagle medium (DMEM) and trypsin were supplied from Thermo Fishner Scientific Inc. (Waltham, MA, USA). The phosphate buffered saline (PBS) and bicinchoninic acid (BCA) protein assay kit were supplied from Solarbio Science & Technology Co., Ltd. (Beijing, China). The puromycin was supplied from Meilunbio (Dalian, China). Fluo-3/AM and pluronic acid F-127 were from Biotium Inc. (Hayward, CA, USA). Insulin and liraglutide were obtained from Novo Nordisk Biotechnology Co., Ltd. (Copenhagen, Denmark). High-performance liquid chromatography (HPLC)-grade methanol, ethanol, acetonitrile and formic acid were from Merck & Co., Inc. (Darmstadt, Germany). Calcium imaging buffer (CIB) of pH 7.2 was prepared by NaCl (7.31 g/L), KCl (0.224 g/L), $MgCl_2$ (0.06 g/L), $NaHCO_3$ (0.10 g/L), $CaCl_2$ (0.55 g/L), HEPES (2.83 g/L), glucose (3.60 g/L) and sucrose (7.21 g/L). Analytes were dissolved in methanol to a concentration of 0.01 M and stored in 1.5 mL EP tubes for chromatographic analysis, and dissolved in dimethyl sulfoxide (DMSO) to make up 0.2 M stock solutions for pharmacological research *in vitro*.

2.2. Cell culture and treatment

Human embryonic kidney 293 (HEK293) cells were purchased from Novabio Scientific Inc. (Shanghai, China). HT22 (mouse hippocampal neuronal cell line) cells were purchased from HyCyte Biotechnology Co., Ltd. (Suzhou, China).

The HEK293 overexpressed GLP-1R (GLP-1R-HEK293) cell line and negative control HEK293 (NC-HEK293) cell line were constructed by lentivirus transfection according to the manufacturer's instructions. The HEK293 cells and HT22 cells were cultured in complete DMEM medium containing 10% FBS, 100 U/mL penicillin and 100 μg/mL streptomycin. And GLP-1R-HEK293 and NC-HEK293 cells were cultured in complete DMEM medium extra adding 2 μg/mL puromycin. All cells were maintained in a 37 °C incubator containing 5% CO_2.

2.3. Preparation of crude Scutellaria baicalensis extract

About 0.3 g of *Scutellaria baicalensis* powder was precisely weighed, then heated reflux extraction with 40 mL 70% ethanol *(V/V)* for 3 h. The mixture was chilled down, filtered with a 0.45 μm membrane and the solution was concentrated to 10 mL by a ZL3-2K vacuum centrifugal concentrator (Changsha, China) at 80 °C. The stock solution of crude *Scutellaria baicalensis* extract was prepared by accurately measuring above concentrated liquor 1 mL and adding methanol to 10 mL, and stored at 4 °C.

2.4. System validation of the GLP-1R/CMC online high-performance liquid chromatography-electrospray-ionization-ion trap-time of flight-multistage (HPLC-ESI-IT-TOF) system

The GLP-1R-HEK293 CMC column was prepared by the protocol recorded before [26]. In brief, GLP-1R-HEK293 cells (1×10^7 cells) were collected, washed, and broken to acquire cell membrane. The GLP-1R cell membrane stationary phase (CMSP) was acquired by blending the cell membrane with pre-activated silica, and following packed into a standard column (10 mm × 2.0 mm I.D.) to prepare GLP-1R/CMC columns. The first dimension was comprised of a GLP-1R/CMC column and a common HPLC system (LC-2030AHT, Shimadzu, Kyoto, Japan) with the following parameters: mobile phase A, water; flow rate, 0.2 mL/min; column oven temperature, 37 °C; and detection wavelengths of UV, 254 nm (BETP) and 278 nm (baicalein). The second dimension was constituted by a liquid chromatography-mass spectrometry (LC-MS) and a matching LC-MS workstation (Shimadzu, Kyoto, Japan). A WondaCr act ODS-2 column was applied to separate complex samples away. A two-position 10-port switching valve (Valco Instrument Co. Inc., Houston, TX, USA) and two RP-18C enrichment columns (10 mm × 4.6 mm; Merck, Darmstadt, Germany) were used to combine the two dimensions together. The system was operated as following parameters: mobile phase A, 0.1% formic acid water (*V/V*); mobile phase B, acetonitrile; gradient procedure, 0−10 min, 8% B; 10.01−25 min, 8%−30% B; 25.01−40 min, 30% B; 40.01−55 min, 30%−50% B; and 55.01−60 min, 50% B; flow rate, 0.8 mL/min. BETP was used as a positive drug to verify the applicability of the two-dimensional (2D) system.

2.5. Frontal analysis

The frontal analysis is a classic method to calculate the equilibrium dissociation constant (K_D value) of the retained components with target receptor, and the concrete procedure has been reported [27]. Briefly, 30%, 40%, 50%, 60%, 70%, 80% and 100% solution B flow through the GLP-1R/CMC column in turn to acquire the breakthrough curves under conditions described below: mobile phases, solvent A (30 mM NaH_2PO_4, pH 7.4), solvent B (10 μM baicalein or 100 μM BETP dissolved in solvent A, pH 7.4); flow rate, 0.2 mL/min; column oven temperature, 37 °C; and detection wavelengths of UV, 254 nm (BETP) and 278 nm (baicalein). At first, solvent A was applied to equilibrate the GLP-1R/CMC column. Then analytes (BETP and baicalein) in a series of concentrations were measured, from lowest to highest proportion. The K_D value was calculated by Eq. (1):

$$\frac{1}{m_{\mathrm{Lapp}}} = \frac{K_D}{m_L} \times \frac{1}{[A]} + \frac{1}{m_L} \tag{1}$$

In Eq. (1), where m_{Lapp} represents the analyte moles at the midpoint of the breakthrough curve under each concentration condition, $[A]$ stands for the molar concentration of analyte, K_D is the dissociation equilibrium constant of analyte, and m_L represents the moles of CMC column binding sites. The K_D value can be calculated by taking the ratio of the slope over the intercept according to Eq. (1) by the linear relationship of $1/m_{\mathrm{Lapp}}$ versus $1/[A]$ [28].

2.6. Non-linear chromatography (NLC)

Due to a variety of sources including extra-column effects, heterogeneity of the stationary phase, heterogenous mass transfer and non-linear isotherm, the actual chromatographic peak profile in liquid chromatography is often asymmetrical. NLC technique is a desired strategy to depict the chromatographic separation procedure occurring on the column, especially when peak tailing existing [29]. The discrepancies of combination and dissociation rates are the primary elements for peak shape. And the peak broadening and the shape deviation often follow non-Gaussian functions [30]. The following equations could formulate the NLC procedure:

$$y = \frac{a_0}{a_3}\Big[1 - exp(-a_3/a_2)\Big]\left[\frac{\sqrt{(a_1/x)}I_1\left(2\sqrt{a_1}x/a_2\right)exp\left[(-x-a_1)/a_2\right]}{1 - T(a_1/a_2, x/a_2)\left[1 - exp(-a_3/a_2)\right]}\right] \tag{2}$$

$$T(u,v) = exp\,(-v)\int_0^u exp(-t)I_0\left(2\sqrt{vt}\right)dt \tag{3}$$

where y represents the detected signal intensity, x stands for the adjusted retention time. The $T(u,v)$ is a switching function to produce peak skew. $I_0()$ and $I_1()$ are modified Bessel functions. Formula (3) plays the conversion function when the chromatographic column is overloaded. The parameters: a_0, a_1, a_2 and a_3 are the best-fit terms applied to fit this equation to the recorded peak shape. The ligand-receptor interaction could be measured as rate constants and equilibrium constant according to following relationships: dissociation rate constant, $k_d = 1/a_2t_0$; binding constant, $K_A = a_3/C_0$; and binding rate constant, $k_a = k_d \times K_A$, where t_0 stands for the column void time and C_0 represents the concentration of injected solute multiplied by the width of the injection. A series of concentrations of BETP and baicalein (0.2, 0.4, 0.6, 0.8, 1.0, 1.2, 1.4, 1.6, 1.8 and 2.0 mM) were analyzed by the GLP-1R/CMC system to study their connection process with GLP-1R. The NLC function in Peak Fit 4.12 was used to process the data.

2.7. Molecular docking study

The crystal structure of GLP-1R (PDB ID: 5VAI) was selected for this docking simulation, and the molecular structures of BETP and baicalein were drawn by ChemDraw 19.0 software and transformed into 3D format by ChemDraw 3D software. Molecular docking was performed by Autodock vina software, and results were visualized by means of Pymol software.

2.8. Live cell fluorescence imaging for Ca^{2+} mobility

GLP-1R-HEK293 cells were seeded in 96-well plates at a density of 5×10^3 per well overnight to adhere to the wall. The cells were washed twice with pre-warmed CIB and then stained with the incubation buffer containing Ca^{2+} fluorescent probe (2.5 μM Fluo-3 AM, 0.1% F-127). After incubation for 40 min, the culture medium was removed and the dyed cells were washed with fresh CIB twice and following immediately imaged under an inverted fluorescence microscope (Nikon, Tokyo, Japan). A series of concentrations of analytes (dissolved in CIB) were added into each well at 5 s after record beginning. Responses were imaged at 3 s intervals for a total of 120 s.

2.9. The enzyme-linked immunosorbent assay (ELISA) measurement for cyclic adenosine monophosphate (cAMP)

GLP-1R-HEK293 cells were cultured in 24-well plates (2×10^4 cell/well) for 48 h, following washed with cold Hank's solution 3 times and incubated in GLP-1 (7–36), liraglutide, BETP or baicalein (10^{-11} ~ 10^{-4} M) for 40 min. After administration, the culture mediums were gathered and centrifuged at 1,000 *g* for 20 min at 4 °C, and the supernatant was collected. Finally, a cAMP enzyme-linked immunosorbent assay (ELISA) kit (Cloud-clone Corp., Wuhan, China) was used to detect cAMP content according to the manufacturer's instructions.

2.10. Mitochondrial membrane potential (MMP) detection

5,5′,6,6′-Tetrachloro-1,1′,3,3′-tetraethyl-imidacarbocyanine iodide (JC-1) (Beyotime Biotechnology, Shanghai, China) staining buffer was applied to evaluate MMP, according to the manufacturer's instructions. Cells were pretreated with high glucose (75 mM) for 1 h followed by administration with 4, 8, 16 and 32 μM of baicalein. After co-incubation for 48 h, 500 μL JC-1 staining work buffer was added to incubate the cells at 37 °C for another 30 min in the dark, where carbonyl cyanide m-chlorophenylhydrazine (CCCP) was used as a positive control. Then cells were washed with pre-cooled PBS, and fluorescence images were subsequently recorded using a fluorescence microscope (Nikon).

2.11. Reactive oxygen species (ROS) level detection

Total ROS of HT22 cells was evaluated using 2′,7′-Dichlorodihydrofluorescein diacetate (DCFH-DA) staining (Solarbio Science & Technology Co., Ltd) according to the manufacturer's instructions. HT22 cells (3×10^3 cells per well) were seeded in a 96-well plate and incubated overnight. Then cells were given with different administrations and further incubated for 48 h. After incubation, the growth medium was removed, and the cells were following stained with DCFH-DA staining buffer (10 μM) at 37 °C for 30 min in the dark. Then cells were washed with pre-warmed hanks balanced salt solution (HBSS; Solarbio Science & Technology Co., Ltd.), and the fluorescence intensity was measured by a FlexStation® 3 multi-mode microplate reader (Sunnyvale, CA, USA) at an excitation wavelength of 504 nm and an emission wavelength of 529 nm.

2.12. RNA interference and transfection

Three small interfering RNAs (siRNAs) targeting *Glp1r* gene were obtained from GenePharma Biotechnology Company (Suzhou,

Table 1
The small interfering RNAs (siRNAs) sequence for glucagon-like peptide-1 receptor (GLP-1R).

	S	AS
siRNA 1	GGCCAGUAGUGUGCUACAATT	UUGUAGCACACUACUACUGGCCTT
siRNA 2	GCAGCCAACUACUACUGGUTT	ACCAGUAGUAGUUGGCUGCTT
siRNA 3	GGCUAUCCUGUACUGCUUUTT	AAAGCAGUACAGGAUAGCCTT

China). The siRNA sequences for *Glp1r* were shown in Table 1.

Cultured HT22 cells were transfected according to following procedure. In brief, cells (2×10^5 per well) were seeded in 6-well plates in DEME medium without FBS and penicillin-streptomycin to grow to 50% confluence. Before transfection, culture medium was removed and cells were washed once with the Opti-MEM medium (Thermo Fisher Scientific Inc.). The siRNAs were dissolved in the Opti-MEM medium to obtain a final concentration of 50 nM, and then mixed with 2 μL Lip2000 transfection reagent (Solarbio Science & Technology Co., Ltd.) to achieve a final volume of 100 μL. The homogeneous mixed solution was standing at room temperature for 20 min, following added to wells together with 900 μL additional fresh Opti-MEM medium. After 6 h incubation, the culture medium was removed and cells were given with 2 mL fresh medium combined with drug administration for 48 h. The efficiency of the siRNAs to silence *Glp1r* gene was determined by Western blots and immunofluorescence analysis.

2.13. Lentiviral vector-mediated overexpression

The human full length gene sequence of *Glp1r* was cloned into a GV358 vector to construct the GV358-GLP-1R recombinant plasmid vector, and following packaged with lentiviruses. The lentiviral particles were used to infect HEK293 and HT22 cells to overexpress *Glp1r* gene, and 2 μg/mL puromycin was applied to screen stable transfected cells out. The transfection efficiency was evaluated by fluorescence intensity, Ca^{2+} mobility and Western blotting assays.

2.14. Animals

In order to investigate the effect of baicalein on T2DM, we performed following protocol. High-fat diet (HFD; Jiangsu Synergy Co., Ltd., Yancheng, China)–fed combined with 60 mg/kg streptozotocin (STZ; Sigma-Aldrich, St. Louis, MO, USA) intraperitoneal injection consecutive 3 days was used to induce T2DM mice model [31]. To be exact, male C57BL/6J wide type (WT) mice weighing 16–20 g were purchased from the Medical Experimental Animal Center of Xi'an Jiaotong University (Xi'an, China). Global *Glp1r* knockout (KO) mice were developed with the Cyagen Bioscience Inc. (Suzhou, China). All mice were housed in a temperature-controlled (23 ± 1 °C) environment with a 12 h light/dark cycle and had free access to diets and water. Mice were randomly sorted into control groups (WT-control and KO-control, $n = 8$) and HFD groups (WT-HFD, $n = 32$ and KO-HFD, $n = 16$) according to body weight (BW). Mice in the control groups were fed with normal chow diets (10% fat, 20% protein and 70% carbohydrates), while mice in the HFD groups were fed with high fat diets (60% fat, 20% protein and 20% carbohydrates). 8 weeks later, after fasting for 12 h, mice in the HFD groups and control groups were intraperitoneally injected with 60 mg/kg BW STZ and isodose citrate buffer respectively for consecutive 3 days. After administration, the fasting blood glucose (FBG) of mice was monitored, the T2DM model was successfully achieved if the FBG of the mice in HFD groups was over 16.7 mmol/L for two consecutive days. Then the WT-HFD mice were randomly divided into 4 groups: Model group and Baicalein groups (50, 100 and 200 mg/kg BW baicalein, respectively, $n = 8$), and the KO-HFD mice were divided into 2 groups: Model group and Baicalein group (100 mg/kg, $n = 8$). The mice in Baicalein groups were intragastric administrated with preestablished dosage of baicalein (dissolved in 0.5% CMC-Na) everyday, while the mice in Control and Model groups were orally administrated with isodose 0.5% CMC-Na. At the end of the 6th week, mice were sacrificed after collecting blood from orbit venous sinus, and the serum was used for biochemical estimation. The hippocampus tissue was removed, gently rinsed in cold saline, quickly frozen in liquid nitrogen and instantly stored at −80 °C for following biochemistry determinations.

All animal experiments in this work were approved by the Institutional Animals Care and Use Committee at Xi'an Jiaotong University and in accordance with the National Institutes of Health Guide for Care and Use of Laboratory Animals (Approval number: SYSK 2020-005).

2.15. Morris water maze (MWM) tests

MWM tests were conducted during the 6th week according to the literature [32], which include spatial probe test for 5 consecutive days and positioning navigation experiment on day 6 to assess the cognitive function of mice. Briefly, on spatial probe test, mice were put into the water facing groove wall at every quadrant, given 90 s to search the hidden platform in the third quadrant, and then allowed to stay on it for 3 s. On the 6th day, the positioning navigation experiment was performed without the platform in the third quadrant for 90 s. The parameters including travel distance, swimming speed, escape latency and platform crossing number were automatically recorded by Taimeng software.

2.16. Western blotting analysis

Proteins extracted from the hippocampus tissue of mice and cultured HT22 cells were used for Western blotting analysis. Briefly, tissue or cells were homogenized and lysed in ice-cold radioimmunoprecipitation assay (RIPA) lysis buffer (Solarbio Science & Technology Co., Ltd.). After ultrasonication and centrifugation, the supernatant was collected, following quantification with the BCA protein assay kit. Ten micrograms of proteins were added to a sodium dodecyl sulfate-polyacrylamide gel electrophoresis (SDS-PAGE) gel (Servicebio Technology Co., Ltd., Wuhan, China) and separated according to molecular weight by electrophoresis. The separated proteins were transferred onto pre-activated polyvinylidene fluoride (PVDF) membranes (Merck Millipore, Darmstadt, Germany). The blots were blocked with 5% (*m/V*) skim milk for 2 h at room temperature, following incubation with primary antibodies overnight at 4 °C. The primary antibodies used were anti-flag (1:1000, Sigma-Aldrich), anti-PGC-1α (1:1000, ABclonal, Wuhan, China), anti-LC3B (1:1000, Proteintech, Wuhan, China), anti-Beclin 1 (1:1000, Proteintech), anti-p62 (1:1000, Proteintech), anti-DRP-1 (1:1000, CST, Boston, MA, USA), anti-MFN-2 (1:1000, CST), anti-GAPDH (1:10000, Proteintech), anti-BDNF (1:1000, CST), anti-PSD95 (1:500, PTM Biolabs, Hangzhou, China) and anti-NeuN (1:1000, CST). After washing three times with Tris-HCl buffered salt solution with Tween 20 (TBST), blots were immersed in horseradish peroxidase (HRP)-conjugated secondary antibodies (1:10000, Proteintech) for 2 h at room temperature, and the membranes were visualized using enhanced chemiluminescence (ECL) HRP substrate reagent (Abbkine, Wuhan, China) by chemiluminescence system (Tanon Life Science Co., Ltd., Shanghai, China).

2.17. Histological analysis of the brain

The brains of mice were acquired and fixed in 4% formaldehyde solution overnight at 4 °C. The paraffin-embedded brains were sectioned into 5-μm thick sections after dehydration and vitrification. The tissue sections were deparaffined with xylene, rehydrated with ethanol in series concentration, and stained with hematoxylin and eosin (HE) (Solarbio Science & Technology Co., Ltd.) or Cresyl violet (Beyotime Biotechnology) staining buffer in proper order. The histopathological microstructure changes of the hippocampus were recorded by an optical positive microscope (Nikon) at 400 × magnification.

2.18. Immunofluorescence

The paraffin-embedded mouse brains were cut into 8-μm thick sections for immunofluorescence staining. Paraffin sections were de-paraffinized in xylene and a series concentration of ethanol, and boiled in 0.01 M citrate buffer for 20 min for antigen retrieval. After cooling down, the sections were permeabilizated with 0.3% Triton X-100 (*V/V*) (Solarbio Science & Technology Co., Ltd.), and following blocked with 5% bovine serum albumin (BSA; Solarbio Science & Technology Co., Ltd.) solution (*m/V*) for 2 h at room temperature. The sections were then incubated with primary antibodies (anti-NeuN and anti-DRP-1, 1:400) overnight at 4 °C. After washed with PBS three times, sections were stained with proper fluorophore-conjugated secondary antibodies (Bioscience Biotechnology Co., Ltd, Shanghai, China) at room temperature for 2 h.

Cells were cultured in 24-well plates on circular glass coverslips (12 mm in diameter) and incubated overnight, and then given with drug administration for 48 h. After washed, cells were fixed in 4% paraformaldehyde, followed by permeabilization, blocking and incubation with antibodies as paraffin sections. For mitochondria imaging, cells were stained with MitoSOX™ Red mitochondrial superoxide indicator (Thermo Fisher Scientific, Ltd.) and mitotracker green (Beyotime Biotechnology). A Zeiss Axioscan Microscopy GmbH (Carl Zeiss AG, Oberkochen, German) was applied for imaging visualization. ImageJ software was used to process and quantify the images.

2.19. Statistical analyses

Data were processed using the GraphPad Prism (version 6.02), and presented as mean ± standard error of mean (SEM) of independent experiments. Statistical analysis between multiple groups were performed using one-way analysis of variance (ANOVA) followed by the least significant difference (LSD) post hoc test, where $P < 0.05$ was recognized as statistically significant, and $P < 0.05$, $P < 0.01$, and $P < 0.001$ shown as *, ** and ***, respectively. Concentration response curves in Ca^{2+} mobility and cAMP accumulation were also fitted using Prism software, according to nonlinear regression analysis (dose-response-stimulation mode). The confocal images exhibited in results are representative pictures of three independent experiments. Parallelly, the immunoblotting data demonstrated in figures are representative of five independent experiments.

3. Results

3.1. Baicalein was screened out as a GLP-1R-targeted compound from Scutellaria baicalensis

The GLP-1R-HEK293 cell line was constructed by lentiviral transfection according to instructions. The detailed plasmid profile applied is shown in Fig. S1A, and the results of pre-experiment for optimizing the condition of transfection in HEK293 cells are shown in Fig. S1B. Western blotting and intracellular Ca^{2+} mobilization assay were applied to detect the GLP-1R expression levels and activity of the transfected cells. The results indicated that GLP-1R protein expression increased almost sixfold in GLP-1R-HEK293 cells compared to HEK293 cells (Fig. S1C), and meanwhile the overexpressed GLP-1R exhibited complete receptor activity, as demonstrated by a significant liraglutide-mediated increase in Ca^{2+} flux in the GLP-1R-HEK293 cells (Fig. S1D). The CMSP consisting of GLP-1R-HEK293 cell membranes and activated silica gel, was packed into a standard column to produce the GLP-1R/CMC column. The results of the system applicability investigation, including selectivity, specificity, column lifetime and reproducibility of GLP-1R/CMC columns, are shown in Fig. S2 and Table S1. The verified GLP-1R/CMC column equipped with HPLC system was coupled with HPLC-ESI-IT-TOF system to formulate the 2D system for fraction separation and identification. BETP, a recognized small-molecule GLP-1R agonist, was used to confirm the validation of the 2D system [33]. As shown in Fig. 1A, the retained fraction R_1 of BETP on GLP-1R/CMC (Fig. 1AI) was enriched and switched into the HPLC-ESI-IT-TOF system (Fig. 1AIII). The chromatogram and the mass spectrometry fragment information, with positive precursor ion at 429.100 mass-to-charge ratio (*m/z*) and optimized product ion at 407.150 *m/z* in Fig. 1AIII showed the same characteristics as the BETP standard reference solution directly analyzed by HPLC-ESI-IT-TOF system (Fig. 1AII). The data shown in Fig. 1A demonstrated that the GLP-1R/CMC-HPLC-ESI-IT-TOF system is applicable for the specific identification of components that interact with GLP-1R.

The validated GLP-1R/CMC-HPLC-ESI-IT-TOF system was applied to screen and identify potential GLP-1R-targeted components from *Scutellaria baicalensis*. The main retention fraction R_1, whose retention time (t_R) is about 10 min, was obtained from the GLP-1R/CMC column (Fig. 1BI), and then switched into the HPLC-ESI-IT-TOF system (Fig. 1BIII), and was identified as baicalein (R_1, molecular weight 271.100). The *Scutellaria baicalensis* extract was also directly injected into the 2D system under the same operation conditions (Fig. 1BII). To further confirm that the components in *Scutellaria baicalensis* binding to GLP-1R was baicalein, the standard reference solution of baicalein was then analyzed using the established system (Fig. 1C). The results confirmed that baicalein exhibited evident retention behavior on GLP-1R/CMC column (Fig. 1CI) and had the same chromatogram (Fig. 1CII) and mass spectrometry fragments (Fig. 1CIII) as R_1 fraction of *Scutellaria baicalensis*.

3.2. Baicalein had stronger binding affinity to GLP-1R than BETP

An agonist's potency can be influenced by its affinity to the receptor. We thus used the frontal analysis method and NLC to determine the binding affinity between the ligands and GLP-1R. The breakthrough curves of BETP (Fig. 2A) and baicalein (Fig. 2B) from 30% B to 100% B were obtained by the frontal analysis method. As shown in left part of Figs. 2A and B, the saturation time of the GLP-1R/CMC column gradually reduced with increasing analyte concentration in the mobile phase. The linear relationship of $1/m_{\mathrm{Lapp}}$ vs $1/[A]$ of BETP and baicalein was obtained from Eq. (1). The fitted lines equations of BETP (Fig. 2A, right) and baicalein (Fig. 2B, right) were $Y = 1.080X + 0.035$ ($r = 0.9965$) and $Y = 1.139X + 1.036$ ($r = 0.9549$), respectively. The K_D values of ligands on the binding site were baicalein (1.099×10^{-7} M) < BETP (3.062×10^{-6} M). To further explore the binding force, NLC was applied. As shown in Figs. 2C and D, the retention time of the analyte gradually increased with decreasing analyte concentration. Using Eqs. (2) and (3), we determined that the binding rate constant k_a was baicalein (5.988 ± 0.752 mol/s) > BETP (5.521 ± 1.013 mol/s), the dissociation rate constant k_d was BETP (1.365 ± 0.497 s^{-1}) > baicalein (0.656 ± 0.038 s^{-1}) and the binding constant K_A was baicalein (10.328 ± 1.635 L/mol) > BETP (5.144 ± 1.234 L/mol). Molecular docking provided details of the interactions between analytes and

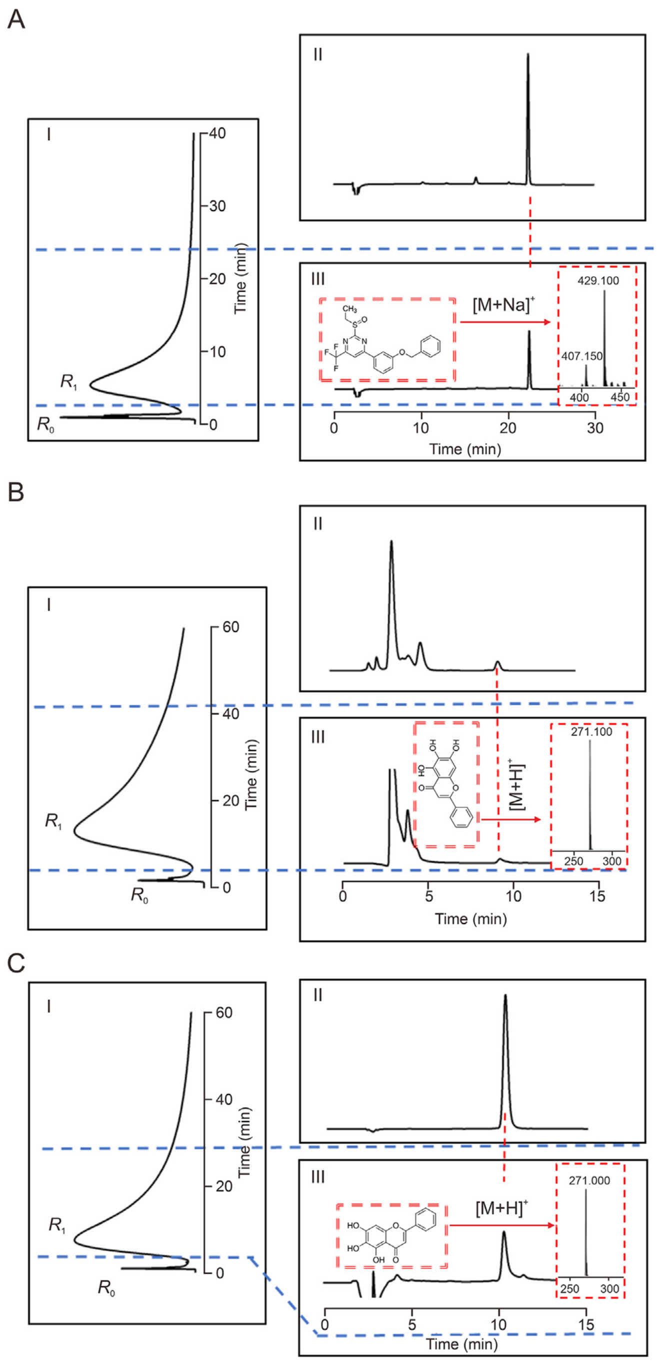

Fig. 1. Baicalein was a glucagon-like peptide-1 receptor (GLP-1R)-targeted component from *Scutellaria baicalensis.* (A) The chromatogram of (4-(3-(Benzyloxy) phenyl)-2-(ethylsulfinyl)-6-(trifluoromethyl) pyrimidine) (BETP) on GLP-1R/cell membrane chromatography (CMC) (I), and high-performance liquid chromatography-electrospray-ionization-ion trap-time of flight-multistage (HPLC-ESI-IT-TOF) system (II), and the chromatogram of retained fraction R_1 on HPLC-ESI-IT-TOF system (III). (B) Chromatogram of the *Scutellaria baicalensis* extract, and its retention record on GLP-1R/CMC (I), and HPLC-ESI-IT-TOF system (II), and the retention fraction R_1 on the HPLC-ESI-IT-TOF system (III). (C) The chromatogram of baicalein standard solution on GLP-1R/CMC (I), and HPLC-ESI-IT-TOF system (II), and the retention fraction R_1 on the HPLC-ESI-IT-TOF system (III). R: retention fraction; M: molecular mass.

GLP-1R at the molecular level. As shown in Figs. 2E and F, BETP and baicalein could form hydrogen bonds with the extracellular domain (ECD) of GLP-1R, while baicalein formed more hydrogen bond amounts with shorter length than the BETP-GLP-1R interaction. The detailed parameters are shown in Table 2. In summary, baicalein had a stronger GLP-1R binding affinity than BETP, reflected by a weaker dissociation rate, a stronger binding rate and more extensive intermolecular hydrogen bonding.

3.3. Baicalein was a potential small-molecule GLP-1R agonist

Ca^{2+} and cAMP are vital intracellular second messengers [34], and both participate in the cellular responses to GLP-1R activation, including rapid Ca^{2+} influx from the extracellular medium and cAMP accumulation [35]. GLP-1(7–36) (Fig. 3A) and liraglutide (Fig. 3B) as GLP-1 analogues facilitated Ca^{2+} mobilization in a dose-dependent manner, with BETP (Fig. 3C) and baicalein (Fig. 3D) showing similar effects. EC_{50} values determined from Ca^{2+} mobilization assay were baicalein (1.129×10^{-7} M) < GLP-1(7–36) (2.279×10^{-7} M) < liraglutide (5.981×10^{-7} M) < BETP (4.751×10^{-5} M). We observed similar results in cAMP accumulation assays (Figs. 3E–H), with EC_{50} values acquired in the order of baicalein (1.458×10^{-9} M) < GLP-1(7–36) (1.180×10^{-8} M) < liraglutide (1.726×10^{-8} M) < BETP (1.539×10^{-7} M).

3.4. Cognitive disorder occurred in diabetes and *Glp1r* KO mice

Cognitive impairment has attracted growing concern as a vital comorbidity of T2DM [36]. We observed a similar association in our research. The spatial memory and learning capacity of diabetes mice in MWM tests were worse than mice in control group, and the cognitive function of *Glp1r* KO mice was found worse than their WT counterparts by accident (Figs. 4A–C). While their athletic ability did not differ significantly between T2DM and control groups (Figs. 4D and E). The protein levels of PSD 95, brain-derived neurotrophic factor (BDNF) and neuronal nuclear antigen (NeuN) in hippocampus tissue of T2DM groups were lower than their corresponding control groups, and *Glp1r* KO brought similar influence on above proteins as HFD/STZ administration (Fig. 4F). HE staining and Nissl's staining results revealed that significant pathological changes had occurred in the hippocampal CA1 region (Fig. 4G). Specifically, the neurons in the WT-control group were intactly and neatly arranged, and the amounts of Nissl body were more than other three groups whose neurons were poorly arranged with unclear profiles. Immunofluorescence histochemical staining of NeuN, a neuron-specific marker, indicated that the number of neurons in the hippocampus, particularly in the CA1 area, was less in T2DM mice and *Glp1r* KO mice compared to the WT-control mice.

3.5. Diabetes mellitus and *Glp1r* KO led to neuronal mitophagy deficiency

Considering the cognitive disorder exhibited in *Glp1r* KO mice, we speculated that GLP-1R might play an important role in the preservation of cognitive function. To find out whether mitophagy is involved in cognitive maintenance, we determined the expression of mitophagy-related proteins in hippocampus tissue of mice subjected to HFD/STZ and *Glp1r* KO. As shown in Fig. 5A, HFD/STZ administration and *Glp1r* KO led to increased p62, decreased Beclin 1 and decreased LC3B-II/I ratio in WT-model mice's brain compared to WT-control mice, indicating autophagy impairment happened. The mitochondrial biogenesis protein PGC-1α and mitochondrial fusion protein MFN-2 decreased, while mitochondrial fission protein DRP-1 increased in T2DM and *Glp1r* KO mice's brains, indicating the occurrence of mitochondrial dynamic disturbance (Fig. 5B). Double immunofluorescent staining revealed that fewer neurons were associated with higher DRP-1 level, suggesting that autophagy impairment and mitochondrial disturbance had occurred simultaneously in cognitive disorder processes of T2DM and *Glp1r* KO mice (Figs. 5C, and S3A and B).

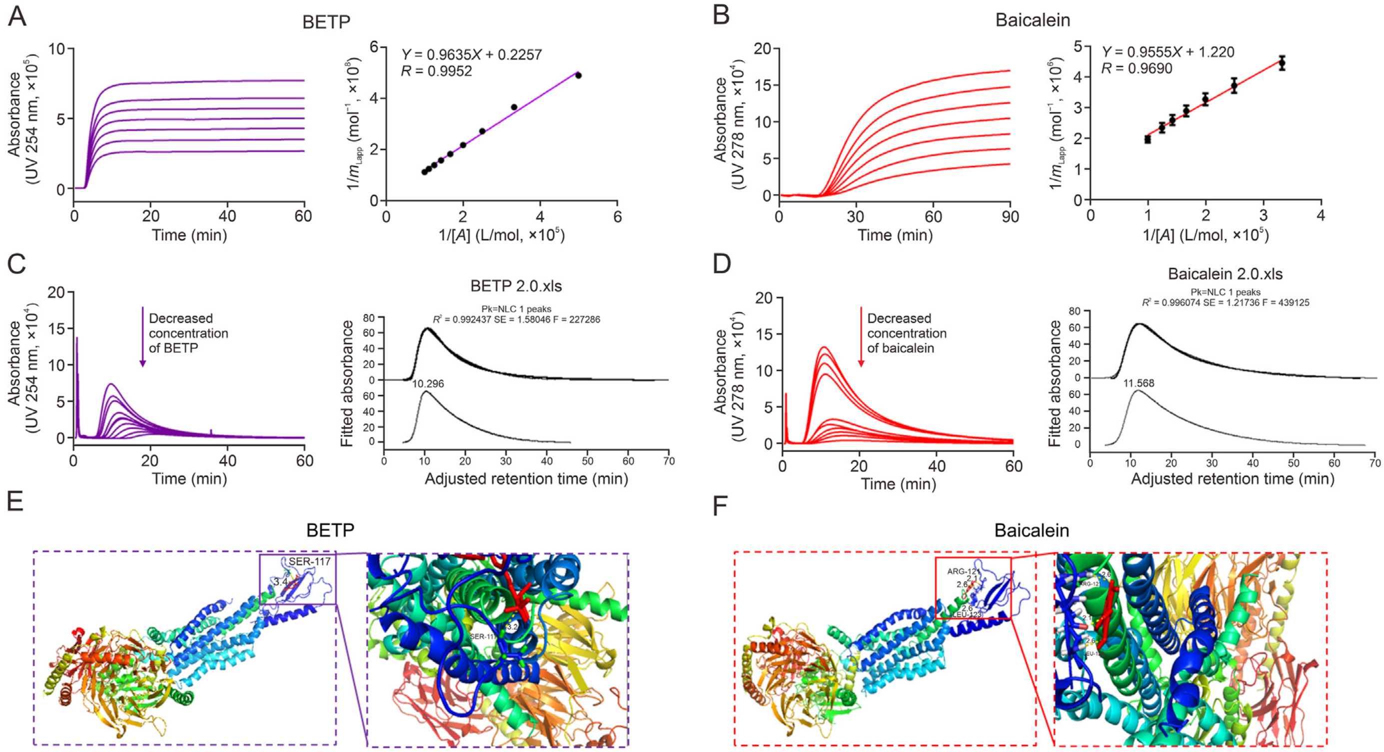

Fig. 2. The binding force analysis of baicalein and 4-(3-(Benzyloxy) phenyl)-2-(ethylsulfinyl)-6-(trifluoromethyl) pyrimidine (BETP) with glucagon-like peptide-1 receptor (GLP-1R). (A) The breakthrough curve (left) and the linear relationship of $1/m_{\mathrm{Lapp}}$ vs $1/[A]$ (right) of BETP on frontal analysis. (B) The breakthrough curve (left) and the linear relationship of $1/m_{\mathrm{Lapp}}$ vs $1/[A]$ (right) of baicalein on frontal analysis. (C) The chromatographic combination chart (left) and fitting curve acquired by Peak Fit 4.12 (right) of BETP on non-linear chromatography (NLC). (D) The chromatographic combination chart (left) and fitting curve acquired by Peak Fit 4.12 (right) of baicalein on NLC. (E,F) Molecular docking results of BETP (E) and baicalein (F) with GLP-1R (PDB ID:5VAI5VAI). $n = 3$ for each group. Data are presented as mean ± standard error of mean (SEM). K_D: the equilibrium dissociation constant; r: linear correlation coefficient.

Table 2
The docking results of small-molecular agonists with glucagon-like peptide-1 receptor (GLP-1R).

Receptor	Ligand	Number of hydrogen bonds	Amino acid residue	Length of hydrogen bonds
5VAI	BETP	1	SER 117	3.4 A
	Baicalein	3	LEU 123	2.6 A
			ARG 121	2.1 A
				2.6 A

SER: Serine; ARG: arginine; LEU: leucine.

3.6. Baicalein ameliorated cognitive dysfunction of T2DM mice in a GLP-1R-dependent manner

The aforementioned results raised the questions regarding the requirement of GLP-1R for cognitive maintenance. To further investigate the therapeutic effect of baicalein, a potential GLP-1R agonist on cognitive disorder of diabetes, we conducted behavioral research on T2DM mice administered with baicalein (Fig. 6A). As shown in Figs. 6B–D, in WT groups, baicalein could improve the cognitive function of T2DM mice compared to their untreated T2DM partners, indicated by the decreased escape latency and increased numbers of platform crossing, while these effects were not observed in *Glp1r* KO mice treated with baicalein. And the differences within WT and KO groups in GLP-1R expression were not significant (Fig. S3C). Baicalein administration had little influence on travel distance and travel speed (Figs. 6E and F). Furthermore, baicalein administration increased the protein levels of PSD 95, BDNF and NeuN in hippocampal tissues of WT-T2DM mice, while such improvement effects were not present in *Glp1r* KO mice administrated with baicalein (Fig. 6G). Taken together, these data indicated that the cognitive disorder improvement effects of baicalein on diabetes were relied on GLP-1R.

To clarify the relationship between the protective effect of baicalein on cognition and mitophagy, we determined mitophagy-related protein levels. As shown in Fig. 7, baicalein had the potential to ameliorate the autophagy decrement and mitochondrial function dysfunction of WT-T2DM mice, while the beneficial effect of baicalein on mitophagy was abolished with *Glp1r* KO. We thus concluded that the neuroprotective effect of baicalein through mitophagy is mediated by GLP-1R.

3.7. Baicalein exerted its neuroprotective effect in HT22 cells by enhancing autophagy and improving mitochondrial dynamics

We established a HT22 cell model under high-glucose (HG) condition *in vitro* to mimic the status of neurons in diabetes, and 75 mM glucose treated 48 h was chosen as the appropriate condition (Fig. S4). As shown in Figs. 8A–D, baicalein had no significant cytotoxicity under 32 μM and could increase the cell viability and MMP, and decrease ROS levels of HG-damaged HT22 cells. As mitochondria are the primary organelle for ROS production, we examined the mitochondrial morphology and ROS levels using mito-tracker green and mitoSOX fluorescence probes, and the results indicated that baicalein decreases the mitochondrial ROS level of HG-damaged HT22 cells (Figs. 8E and S5A). Whereas there were no significant differences in GLP-1R protein expression between the groups, indicating that the beneficial effect described above was not induced by changes in GLP-1R expression level (Figs. 8F and S5B).

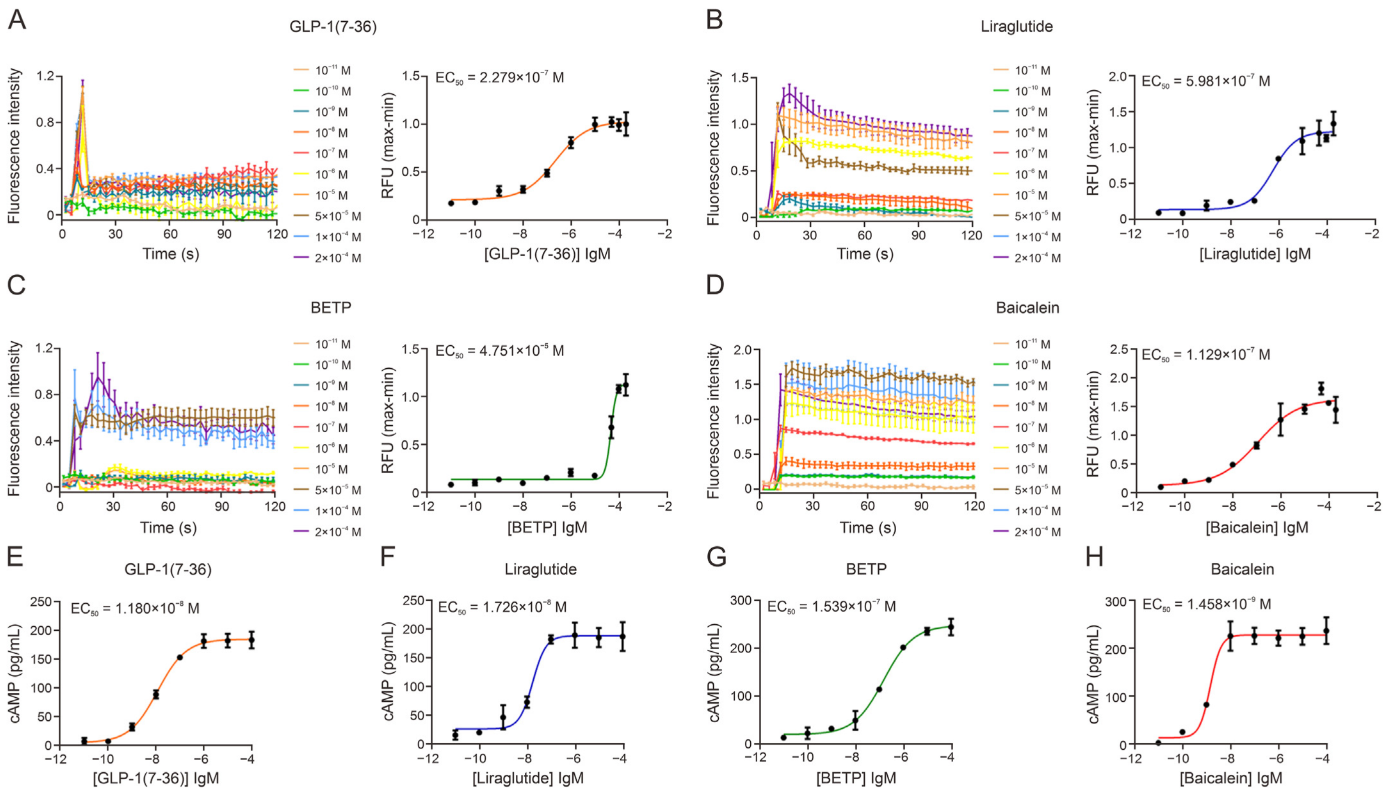

Fig. 3. Glucagon-like peptide-1 receptor (GLP-1R) activation effect analysis of GLP-1analogues, 4-(3-(Benzyloxy) phenyl)-2-(ethylsulfinyl)-6-(trifluoromethyl) pyrimidine (BETP) and baicalein. (A–D) The effects of GLP-1(7–36) (A), liraglutide (B), BETP (C), and baicalein (D) on Ca^{2+} mobilization of GLP-1R-HEK293 cells. Graphs on the left represent the curve of fluorescence intensity and time, and on the right are quantification of the relative fluorescence intensity changes (n = 6). (E–H) The effects of GLP-1(7–36) (E), liraglutide (F), BETP (G), and baicalein (H) on cAMP (cyclic adenosine monophosphate) accumulation assay ($n = 3$). Data are presented as the mean ± standard error of mean (SEM). HEK293: human embryonic kidney 293; RFU: relative fluorescence intensity changes.

To verify the involvement of baicalein in autophagy improvement, we determined the protein levels of LC3B, p62 and Beclin 1 in HT22 cells. The results indicated that baicalein compensates the autophagy deficiency of HT22 cells caused by HG (Figs. 8G and S5C). We acquired similar results in immunofluorescence colocalization of LC3B and mitochondria (Figs. 8H and S5D). To confirm the beneficial effect of baicalein on mitochondria, we examined the protein levels of PGC-1α, MFN-2 and DRP-1. The results showed that under HG conditions, the expressions of PGC-1α and MFN-2 are significantly downregulated, while DRP-1 expression is clearly upregulated, and baicalein has the potential to reverse these trends (Figs. 8I and S5E). These results suggested that baicalein produces significant neuroprotective effects against HG damage by enhancing autophagy and improving the mitochondrial dynamics of HT22 cells.

3.8. *Baicalein rescued mitophagy deficiency against HG in a GLP-1R-dependent manner*

To further investigate the relationship between GLP-1R and the neuroprotective effects of baicalein described above, we used siRNA and lentiviral vector to knock down and overexpress the GLP-1R. We implemented a pre-experiment to determine the optimum siRNA sequence for GLP-1R knock down. As shown in Fig. S6, the siRNA3 demonstrated the best knockdown efficiency and thus was applied in subsequent experiments.

Mitochondrial dysfunction often caused by impaired fusion and hyper-functional fission, inducing mitochondria exhibited in particle shape. And with mitochondrial function recovery, the mitochondrial morphology exhibited in extension profile. Our results indicated that the beneficial effects of baicalein on enhancing mitochondrial fusion and autophagy, decreasing mitochondrial fission and mito-ROS were discounted with *Glp1r* knockdown (Figs. 9A–C and S7A). Besides, under HG conditions, mitochondria were in fragmented structure, and baicalein had the potential to recover it into extensional form, while *Glp1r* knockdown could counteract its beneficial effects (Figs. 9D and S7B). Furthermore, *Glp1r* overexpression decreased mitochondrial fission and ROS, enhancing mitochondrial fusion (Figs. 9E–G and S7C). The mitochondria fluorescence imaging results indicated that *Glp1r* overexpression contributes it to exhibit in filamentous network structure (Figs. 9H and S7D). The all indicated that baicalein could rescue mitophagy deficiency against HG in a GLP-1R-dependent manner.

4. Discussion and conclusion

Baicalein, a kind of flavonoid compounds, exists abundantly in esculent medicinal plants, such as *Scutellaria baicalensis Georgi* and *Oroxylum indicum (L.) Kurz* [37]. Flavonoids, possessing a common chemical structure (C6-C3-C6) and a natural ability to inhibit α-glucosidase activity, have drawn widespread attentions in the field of hypoglycemic drugs research and development [38]. Researches on baicalein have confirmed that it can modulate endoplasmic reticulum (ER) stress [39], inhibit α-glucosidase activity [40], play anti-oxidant and anti-inflammatory roles [41,42], and thus act to decrease blood glucose and lipids. In this work, chromatographic science, molecular biology and molecular docking simulations were applied to demonstrate that baicalein is a potential GLP-1R small-molecule agonist.

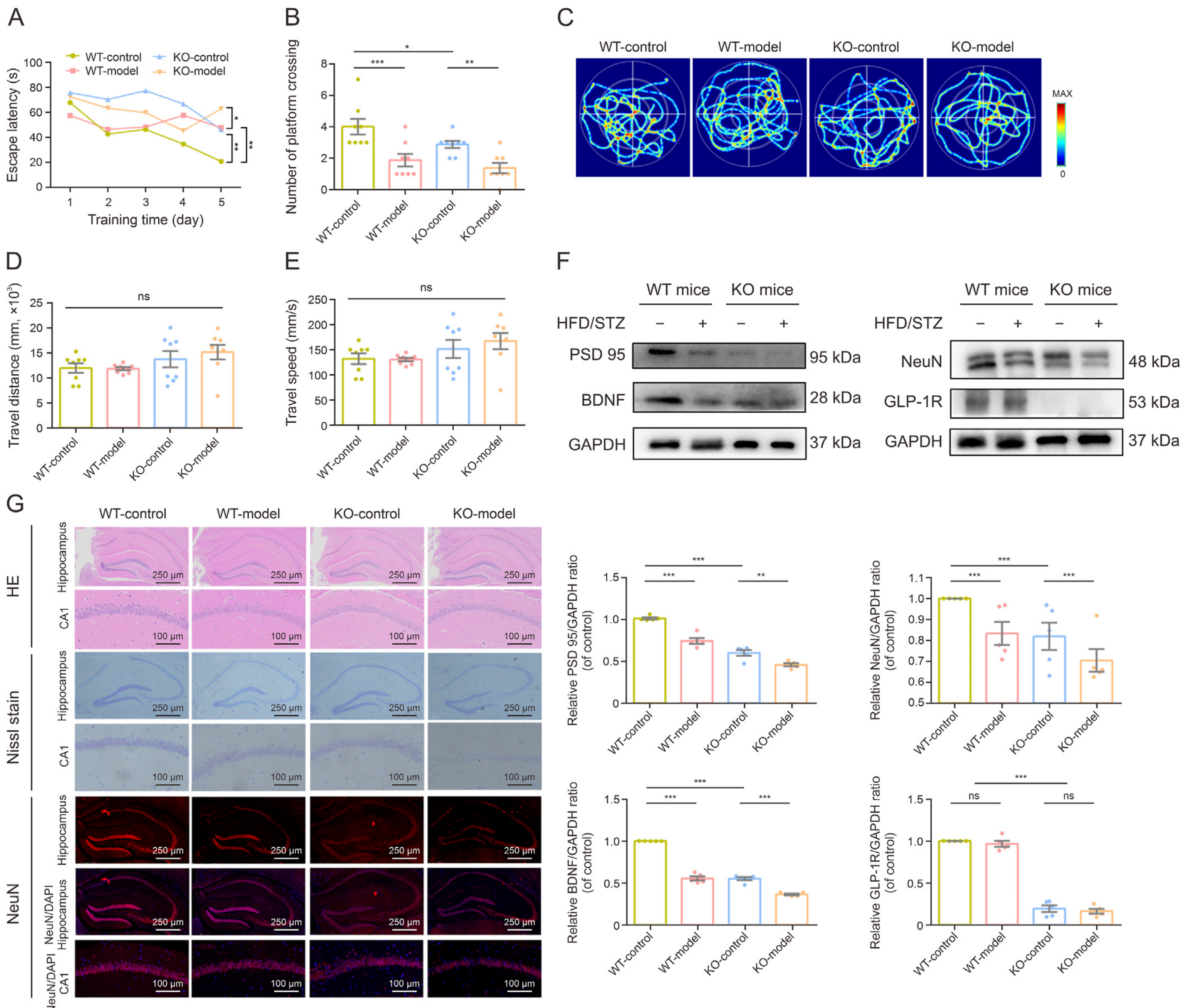

Fig. 4. Cognitive disorder occurred in type 2 diabetes mellitus (T2DM) and glucagon-like peptide-1 receptor (*Glp1r*) gene knockout (KO) mice. (A–C) The mean escape latency (A), number of platform crossing (B), and (C) representative traces (C) of mice subjected to positioning navigation experiment in Morris water maze (MWM) assay. (D) Travel distance and (E) travel speed. $n = 8$ for each group. (F) Representative Western blotting bands of post-synaptic density protein 95 (PSD 95), brain-derived neurotrophic factor (BDNF), neuronal nuclear antigen (NeuN) and GLP-1R expression levels in hippocampus of mice (upper) and quantification of PSD 95/glyceraldehyde-3-phosphate dehydrogenase (GAPDH), BDNF/GAPDH, NeuN/GAPDH and GLP-1R/GAPDH in the mice hippocampus tissue among different groups (below). $n = 5$ mice for each group. Data are presented as mean ± standard error of mean (SEM). (G) The histological stain of hematoxylin and eosin (HE) (upper), Nissle (middle) and NeuN (below) in hippocampus and CA1 area in hippocampus of mice brain slice. Data are presented as mean ± standard error of mean (SEM). $^{*}P < 0.05$, $^{**}P < 0.01$, $^{***}P < 0.001$; ns: no significance. One-way analysis of variance (ANOVA) with Tukey's post hoc test. WT: wide type; HFD: high fat diet; STZ: streptozotocin.

Eriodictyol, luteolin, morin, myricetin and quercetin are structural analogues to baicalein, owing to the presence of a similar aromatic stem nucleus (Fig. S8). Myricetin, a kind of flavonoids, is characterized by a pyrogallol B-bring and has been identified as a potential natural GLP-1R agonist that can be orally administered. Besides, myricetin exhibits enhanced biological properties due to its more extensive hydroxylation compared to other flavonols [43,44]. Quercetin [45], luteolin [46], morin and eriodictyol also have exhibited anti-diabetic pharmacological activity [47,48], primarily based on their anti-oxidant effects. However, there were few studies clarify the connection between the activity of these compounds and GLP-1R. Here we attempted to clarify the correlation of the improvement effect of these compounds with GLP-1R through preliminary docking (Table S2 and Fig. S9), where ECD of GLP-1R has been described to form a distinct conformation that might have profound effects on partial agonism and biased signal transduction of GLP-1R agonists [17]. Hydrogen bonding is considered the most important noncovalent interaction in biological recognition processes. Hydrogen bonds formed by small-molecule drugs with their protein targets are predominantly mediated by hydroxyl groups on the drugs. Thus, the number of hydrogen bonds in such interactions correlates with the extent of hydroxylation. The pharmacokinetic properties of drugs are partly dependent on their electrophilic nature [19], while the receptor agonism effect depends on a range of factors, such as compound structure, hydrophilicity, lipophilicity and the potential of ligands to trigger metastasis of the ECD from the transmembrane domain (TMD).

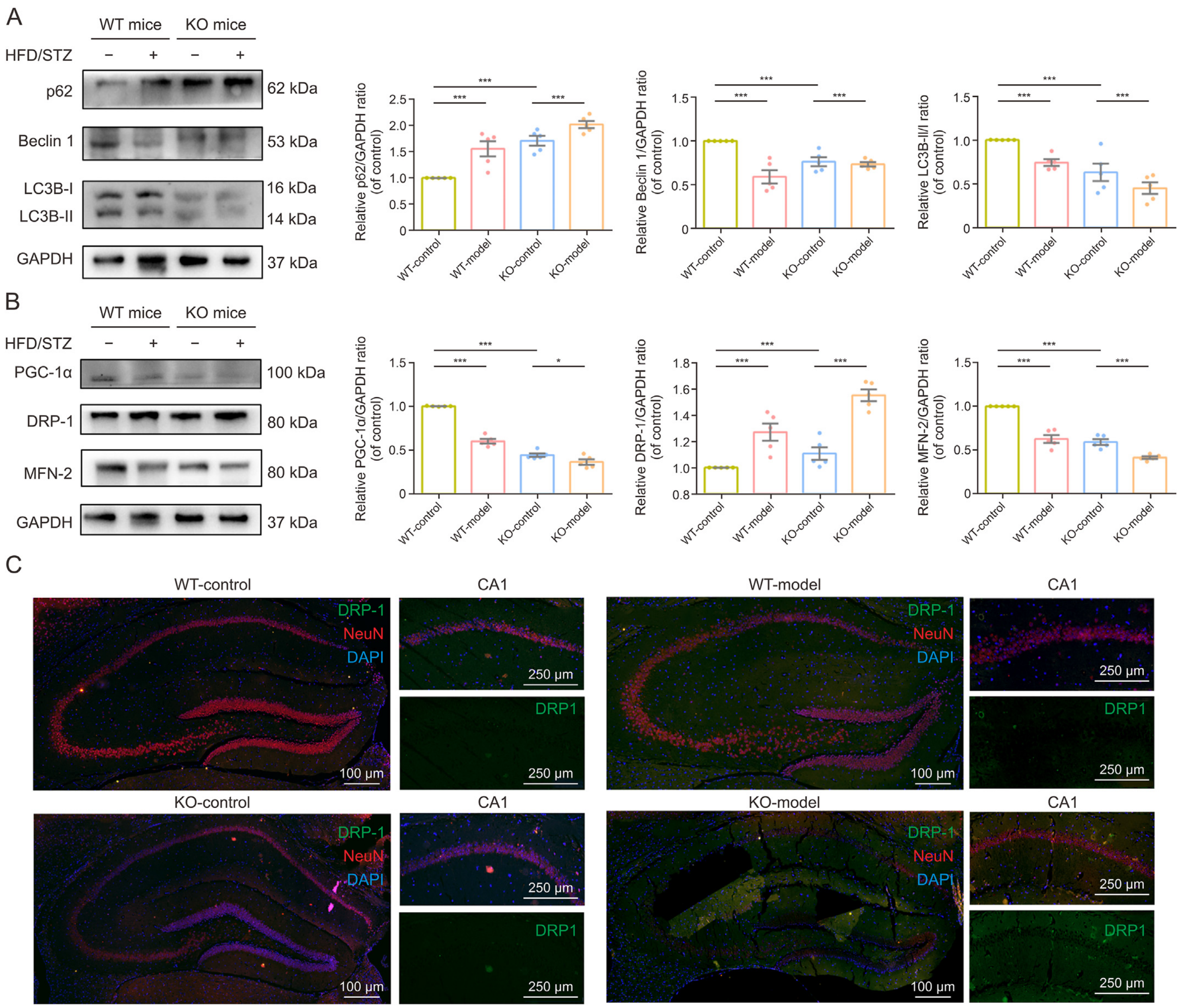

Fig. 5. Mitophagy deficiency took place in type 2 diabetes mellitus (T2DM) and glucagon-like peptide-1 receptor (*Glp1r*) *gene* knockout (KO) mice. (A) Representative Western blots bands of p62, Beclin 1, noncanonical light chain 3B (LC3B) expression in hippocampus tissue of mice (left) and quantification of p62/glyceraldehyde-3-phosphate dehydrogenase (GAPDH), Beclin 1/GAPDH, and LC3B-II/I ratio among different groups (right). (B) Representative Western blots bands of peroxisome proliferator-activated receptor-γ coactivator (PGC)-1α, dynamin-related protein 1 (DRP-1) and mitofusin-2 (MFN-2) expression levels in hippocampus of mice (left), and quantification of proteins mentioned above to GAPDH (right). $n = 5$ for each group. (C) The brain slices were stained with neuronal nuclear antigen (NeuN) (red), Drp-1 (green) and 4′,6-diamidino-2-phenylindole (DAPI) (blue) (complete co-localization) in the whole hippocampal region (left), hippocampal CA1 region (upper right) and DRP-1 stain in hippocampal CA1 region (low right). Data are presented as mean ± standard error of mean (SEM). $^{*}P < 0.05$, $^{***}P < 0.001$. One-way analysis of variance (ANOVA) with Tukey's post hoc test. p62: p62/SQSTM1; WT: wide type; HFD: high fat diet; STZ: streptozotocin.

An alternative approach to GLP-1 peptide mimetic therapy is the use of positive allosteric modulators (PAMs) that can bind to sites other than the ligand-binding pocket, which could induce a conformational change in the ECD. That makes it enter into the orthosteric pocket via its N-terminus, and enhances agonist's activity [49]. PAMs, such as BETP, an electrophilic chemotype compound, and compound 2 (6,7-dichloro-3-methanesulfonyl-2-tert-butylamino-quinoxaline), a substituted quinoxaline, require an intact ECD to sponsor or trigger receptor activation [33,50]. Compound 2 triggers the outward movement of TM6 in cooperation with the ECD whose N terminus penetrates into the GLP-1 binding site through forming predominantly hydrophobic interactions with the adjacent residues in TM6 [51]. Taken together, the analysis of structure-activity relationships is of vital importance for understanding receptor activation and might provide new insights for non-peptide GLP-1R agonist development.

Although insulin resistance or insufficiency remains the principal hallmark of diabetes mellitus, emerging evidence has highlighted the importance of cognitive abnormalities [52]. Indeed, the risk of dementia is significantly increased in diabetic versus non-diabetic individuals [53]. Although several pathological processes are known to be involved in the progress of cognitive decline, the detailed underlying molecular mechanisms require further clarification. An elevated plasma glycated haemoglobin (HbA1c) level is correlated with cognitive decline, indicating that glucose maladjustment alone is enough to induce cognitive impairment [54]. It is well-established that persistent hyperglycemia can trigger microvascular and macrovascular changes in diverse organs, including

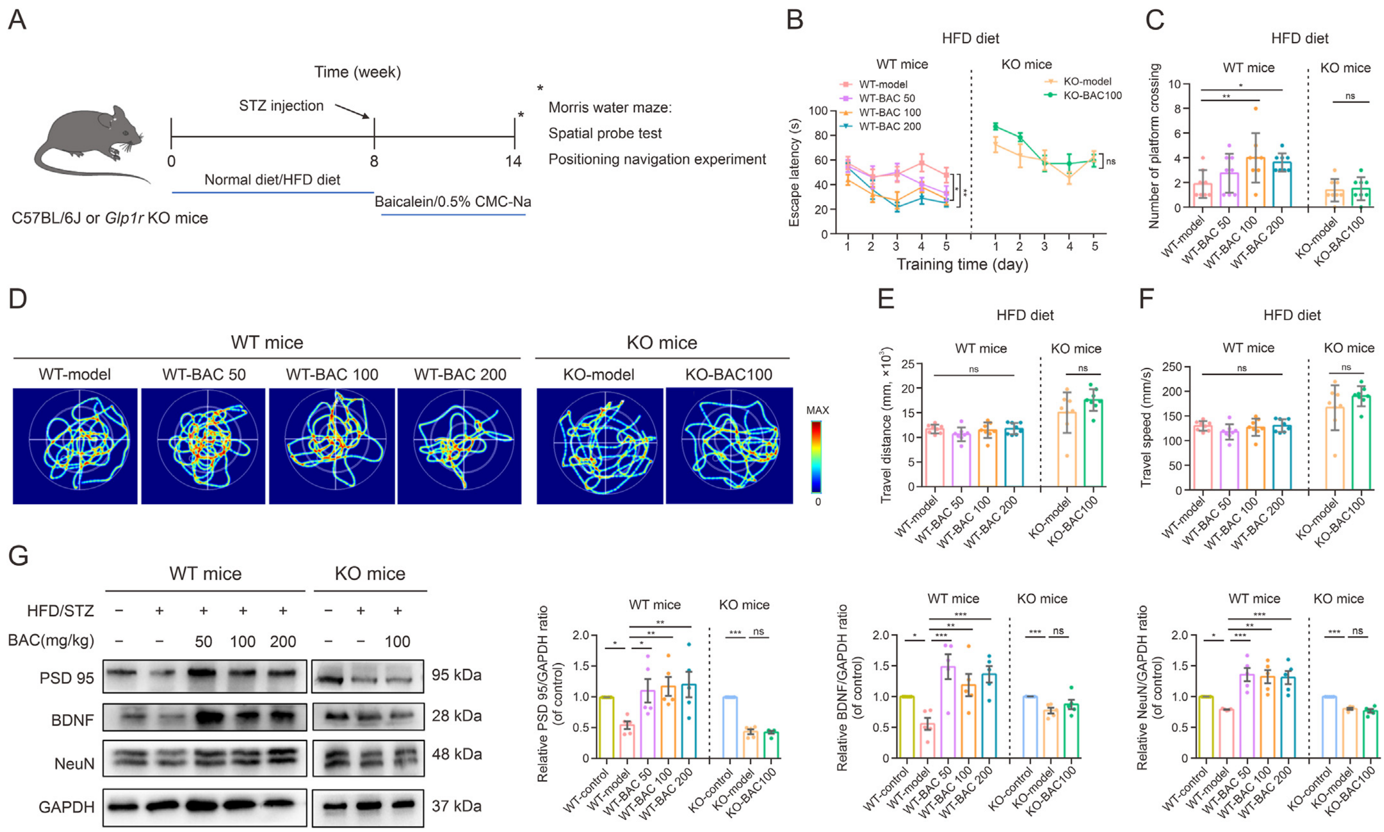

Fig. 6. Baicalein (BAC) improved cognitive disorder of type 2 diabetes mellitus (T2DM) mice in a glucagon-like peptide-1 receptor (GLP-1R)-dependent way. (A) Schematic of T2DM mice model construction and drug administrations in wide type (WT) and *Glp1r* knockout (KO) mice. (B–D) The mean escape latency (B), number of platform crossing (C), representative traces (D) of T2DM mice on positioning navigation experiment subjected to Morris water maze (MWM) assay. (E) Travel distance and (F) travel speed. $n = 8$ for each group. (G) Representative of Western blots bands for post-synaptic density protein 95 (PSD 95), brain-derived neurotrophic factor (BDNF), and neuronal nuclear antigen (NeuN) in the hippocampus of each group mice (left) and quantitative analysis of those protein levels (right). $n = 5$ mice for each group. Data are presented as mean ± standard error of mean (SEM). $^{*}P < 0.05$, $^{**}P < 0.01$, $^{***}P < 0.001$; ns: no significance. One-way analysis of variance (ANOVA) with Tukey's post hoc test. STZ: streptozotocin; HFD: high fat diet; GAPDH: glyceraldehyde-3-phosphate dehydrogenase.

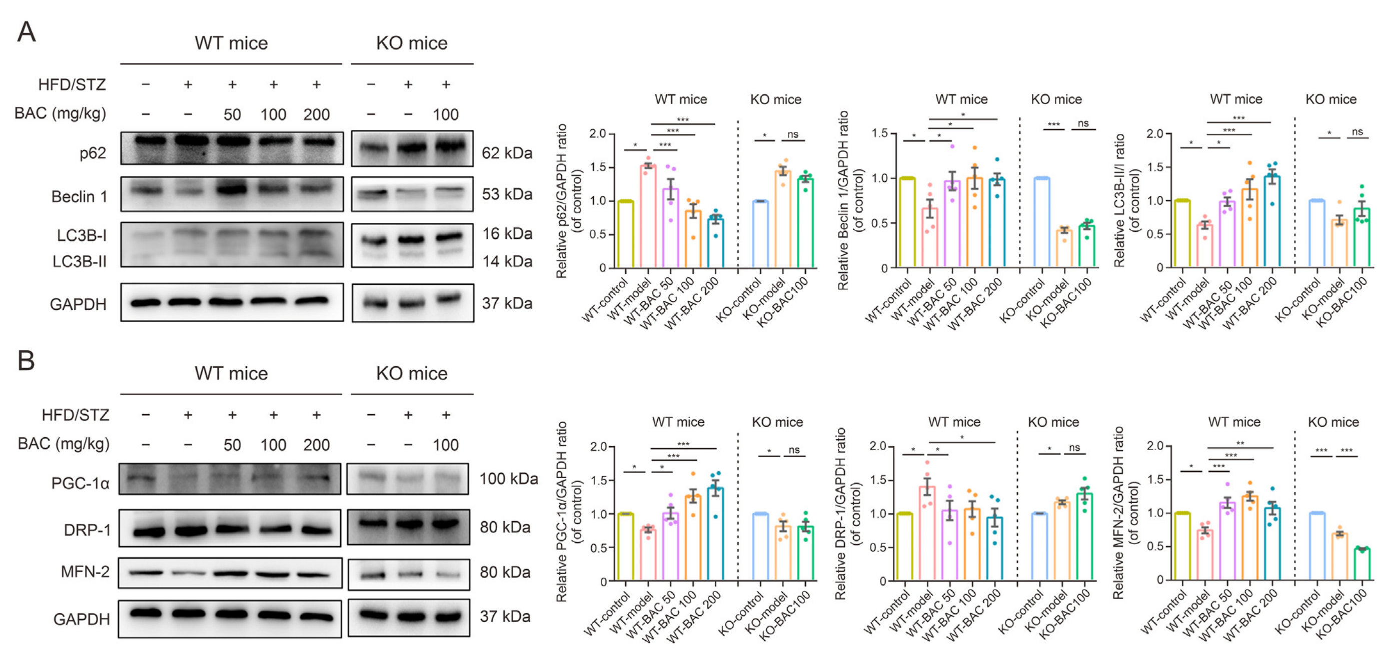

Fig. 7. Glucagon-like peptide-1 receptor (*Glp1r*) knockout (KO) counteracted the beneficial effect of baicalein on mitophagy in hippocampus tissue of mice. (A) Representative bands of Western blots and quantification of noncanonical light chain 3B (LC3B), p62 and Beclin 1 levels in the hippocampus of each group mice. (B) Representative bands of Western blots and quantification of peroxisome proliferator-activated receptor-γ coactivator (PGC)-1α, dynamin-related protein 1 (DRP-1) and mitofusin-2 (MFN-2) levels. $n = 5$ mice for each group. Data are presented as mean ± standard error of mean (SEM). $^{*}P < 0.05$, $^{**}P < 0.01$, $^{***}P < 0.001$; ns: no significance. One-way analysis of variance (ANOVA) with Tukey's post hoc test. p62: p62/SQSTM1; BAC: baicalein; WT: wide type; STZ: streptozotocin; HFD: high fat diet; GAPDH: glyceraldehyde-3-phosphate dehydrogenase..

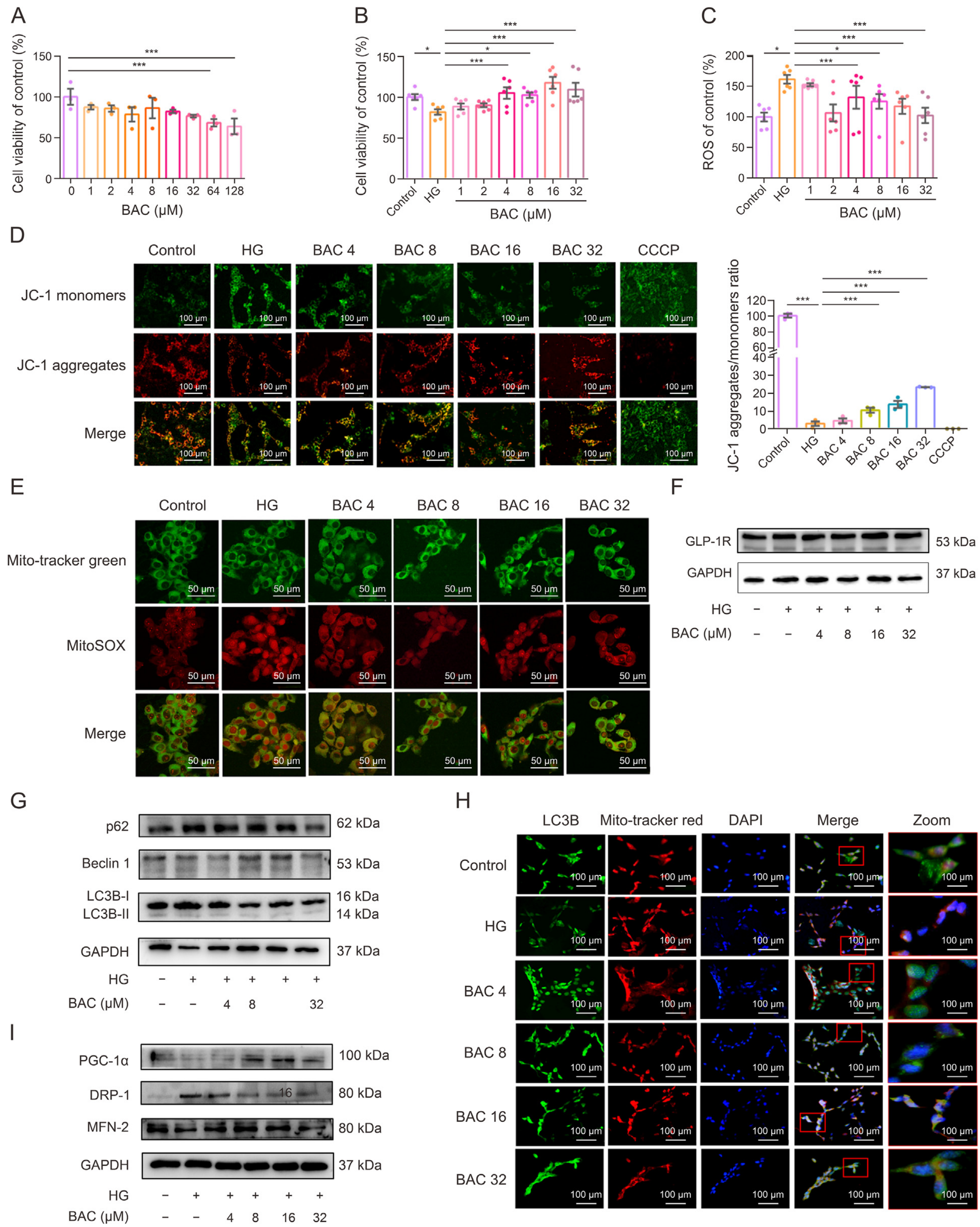

Fig. 8. Baicalein (BAC) played the neuroprotective effect through enhancing mitophagy of HT22 cells. (A) The cell viability of HT22 cells administrated with different concentrations of BAC determined by (3-(4,5-dimethylthiazol-2-yl)-2,5-diphenyltetrazolium bromide) tetrazolium (MTT) assay. $n = 3$ for each group. (B) The cell viability of HT22 cells given with high glucose (HG) and different concentrations of BAC administration. $n = 6$ for each group. (C) Reactive oxygen species (ROS) level detected by dichloro-dihydro-fluorescein diacetate (DCFH-DA) probe in different groups. $n = 6$ for each group. (D) 5,5′,6,6′-Tetrachloro-1,1′,3,3′-tetraethyl-imidacarbocyanine iodide (JC-1) staining for mitochondrial membrane potential (MMP) performed in HT22 cells (left) and quantification of fluorescence intensity (right). $n = 3$ for each group. (E) Fluorescence colocalization of mitochondrial morphology (green) and mitochondrial reactive oxygen species (mito-ROS) (red) in different groups. (F) Representative Western blots band for glucagon-like peptide-1 receptor (GLP-1R) expression in HT22 cells given with HG and BAC administration. (G) Representative Western blots bands for autophagy-related protein. (H) Immunofluorescence for colocalization of light chain 3B (LC3B) (green), mitochondrial ROS (red) of HT22 cells. (I) Representative Western blots bands for mitochondrial dynamics-related protein. Data are presented as mean ± standard error of mean (SEM). $^{*}P < 0.05$, $^{***}P < 0.001$. One-way analysis of variance (ANOVA) with Tukey's post hoc test. PGC-1α: peroxisome proliferator-activated receptor-γ coactivator-1α; DRP-1: dynamin-related protein 1; MFN-2: mitofusin-2; CCCP: carbonyl cyanide m-chlorophenylhydrazine; DAPI: 4′,6-diamidino-2-phenylindole; GAPDH: glyceraldehyde-3-phosphate dehydrogenase.

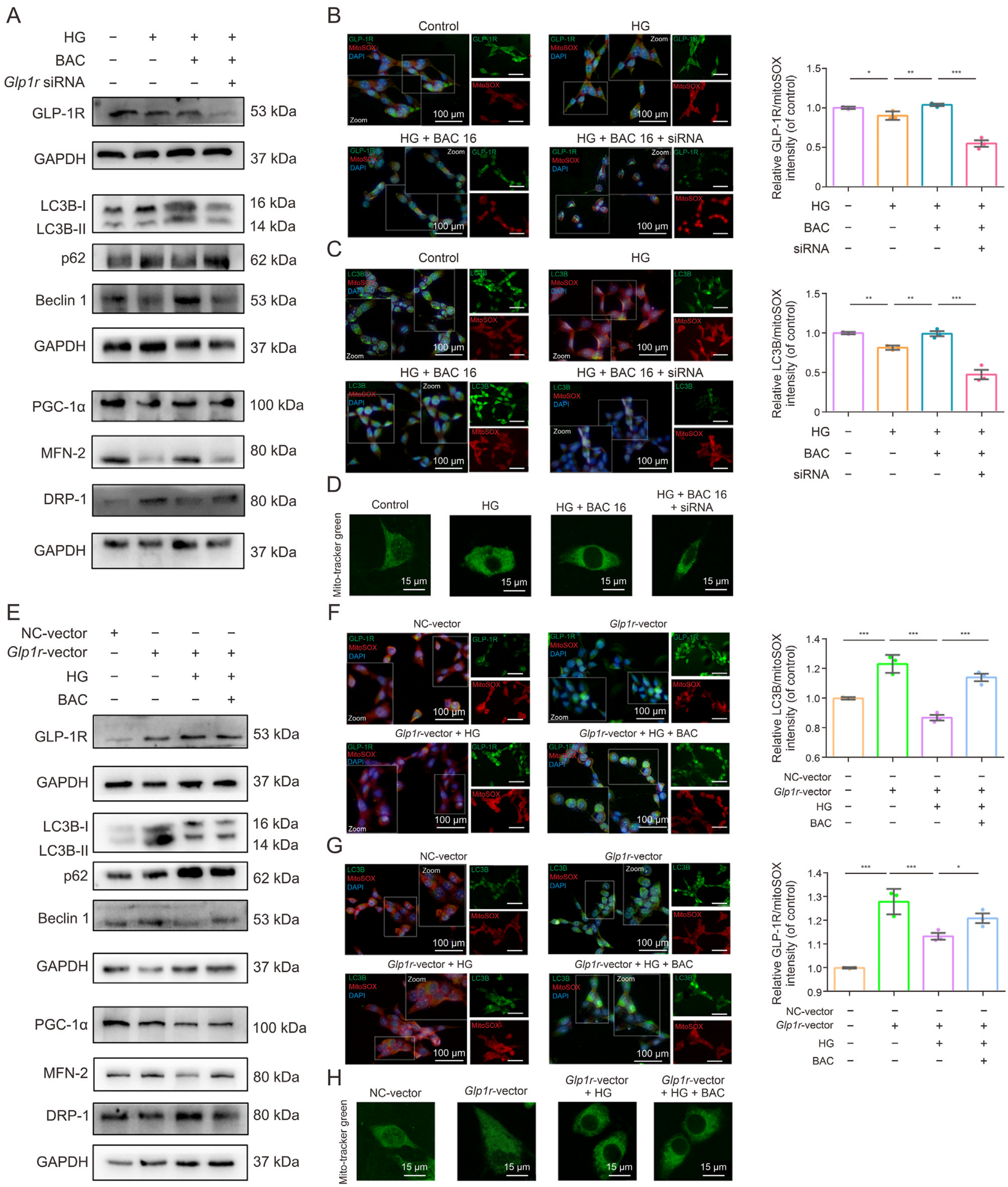

Fig. 9. Baicalein (BAC) rescued mitophagy deficiency against high glucose (HG) in a glucagon-like peptide-1 receptor (GLP-1R)-dependent manner. (A, E) Representative Western blots band for GLP-1R, light chain 3B (LC3B), p62, Beclin 1, peroxisome proliferator-activated receptor-γ coactivator (PGC)-1α, dynamin-related protein 1 (DRP-1) and mitofusin-2 (MFN-2) expression in HT22 cells given with different administrations. (B, F) Immunofluorescence for colocalization of GLP-1R (green) and mitochondrial reactive oxygen species (mito-ROS) (red) in different groups (left) and quantitative analysis results (right). n = 3 for each group. (C, G) Immunofluorescence for colocalization of LC3B (green) andmito-ROS (red) in different groups. Scale bar, 100 μm. (D, H) Fluorescence staining of mitochondrial morphology by mito-tracker green probe. Data are presented as mean ± standard error of mean (SEM). $^{*}P < 0.05$, $^{**}P < 0.01$, $^{***}P < 0.001$. one-way analysis of variance (ANOVA) with Tukey's post hoc test. NC: negative control; GAPDH: glyceraldehyde-3-phosphate dehydrogenase.

the brain [55]. Furthermore, AD-like pathological changes, such as amyloid β (Aβ) deposition and the presence of islet amyloid polypeptide (IAPP) have been detected in the brain of people with diabetes, leading to aggregated pancreatic islet amyloid, which is

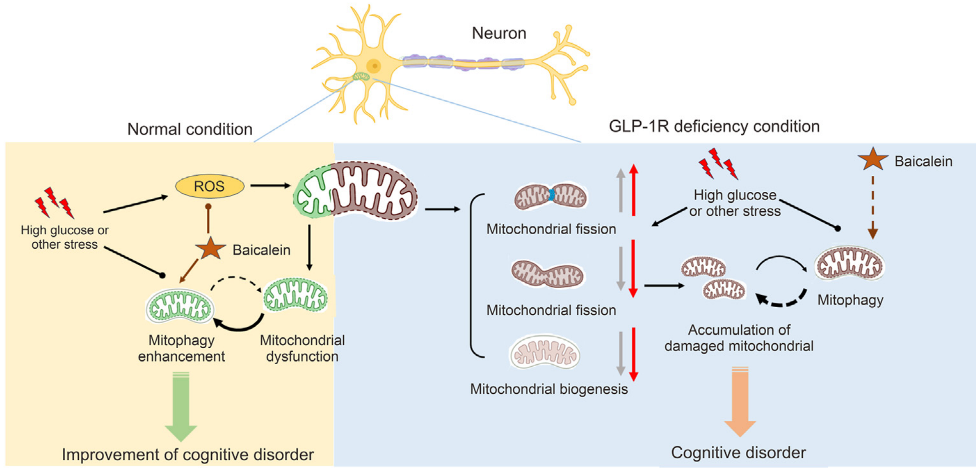

Fig. 10. Baicalein improves cognitive disorder of diabetes through enhancing mitophagy under the existing of glucagon-like peptide-1 receptor (GLP-1R). On the normal condition, reactive oxygen species (ROS) level increasing with the stimulation of stress, such as high glucose and diabetes microenvironment, which induce mitochondrial dysfunction, including augmentation of mitochondrial fission level, attenuation of mitochondrial fusion and impairment of mitochondrial biogenesis. Mitophagy, taking important part in eliminating damaged mitochondria and regulating mitochondrial quality, is also impaired with stress stimulation. The all causes cognitive disorder directly and indirectly. Baicalein comes into play not only decrease ROS level, but also enhance mitophagy directly, which is a gospel for cognitive disorder. While with the GLP-1R knockout, the role of baicalein on mitophagy is abolished. Following that is accumulation of damaged mitochondria, imbalanced mitochondrial control system and coming cognitive disorder recklessly.

the indication of cognitive decline. This effect is partially attributable to heterologous interactions between IAPP and human Aβ, which has an overall amino acid sequence identity of 25% and an even higher degree of similarity in regions that mediate fibril formation. IAPP and Aβ also share many biophysical and physiological properties and exert similar cytotoxic effects when aggregated [56]. These factors are consistent with the beneficial effect of antidiabetic drugs on cognitive impairment associated with diabetes. GLP-1RAs, as novel hypoglycemics, could inhibit glucagon secretion, food intake and gastric emptying, and have been applied to the therapy of diabetes and obesity [57]. Emerging studies have shown that GLP-1RAs have additional beneficial effects on promoting cognitive function of diabetic subjects. Notwithstanding, other potential molecular mechanisms are yet to be identified, several possible pathways may be responsible for these positive effects, including attenuating neuroinflammation [58], antioxidative properties in neuronal networks [59], mimicking and promoting insulin signaling [60], lowering the neuroapoptosis [61], lowering glucotoxicity [62], deferring Aβ and tau proteins aggregation [63], inducing neurogenesis, synaptogenesis and long-term potentiation (LTP) formation/potentiation [64] and maintaining natural structures, functions and metabolic homeostasis of neurons [65]. Apropos of this, our research directly verified the importance of GLP-1R on cognitive function. As *Glp1r* KO mice displayed significant cognitive impairment symptoms, baicalein administration could only improve the cognitive disorder of diabetes mice in the presence of GLP-1R.

Dysfunctional mitochondria also contribute to the pathogenesis of cognitive disorders, reflected by the size increase and dysfunctional mitochondria observed in the brain of cognitive impaired rodents [66]. Numerous studies have revealed that GLP-1R activation has profound beneficial effects on learning and memory recovery in multiple diseases [67–69]. Mitochondria are nutrient sensors that play pivotal roles in modulating central energy and glucose homeostasis [70]. Autophagy plays an important role in mitochondrial quality control [71]. Mitophagy, a selective autophagy subroutine targeted toward damaged and potential detrimental mitochondria, helps to improve mitochondrial quality and running efficiency [72]. Neuronal mitochondria contribute to the regulation and control of central and general energy metabolism, and their imbalance can induce cognitive disorder [73–75]. DA4-JC, a GLP-1/GIP dual receptor agonist, improved cognitive impairment of an APP/PS1/tau mouse model of AD through improvement of the putative kinase 1 (PINK 1)–Parkin mitophagy signaling pathway [13]. Furthermore, researchers also found that exendin 4, a GLP-1RA, could modulate depression-like behaviors in diabetic mice through inhibiting microglial pyroptosis via promotion of mitophagy [76]. We suspected that the activation of GLP-1R might play a neuroprotective effect via the enhancement of mitophagy in multi-cognitive disorder diseases. The results of our research intuitionally explicated the importance of GLP-1R on mitochondrial homeostasis. PGC-1α expression was significantly decreased in *Glp1r* KO mice, indicating that the biogenesis of mitochondria was impaired with the abolishment of GLP-1R, while baicalein increased the expression of PGC-1α in a GLP-1R-dependent manner. Furthermore, the elevated DRP-1 and decreased MFN-2 levels were consistent with the imbalance of mitochondrial quality control in T2DM and *Glp1r* KO mice. Our further research on HT22 cells indicated that the overexpression of GLP-1R was able to significantly enhance the mitochondrial quality control. Consistent with *in vivo* assays, the GLP-1R knockdown counteracted such beneficial effects of baicalein on mitochondria of HT22 cells.

Researches on the relationship between cognitive decline and GLP-1R are limited. In our research, we found that the cognitive function of *Glp1r* KO mice was significantly impaired, both in KO-T2DM group and KO-control group. While, baicalein administration had little influence on GLP-1R expression. Taken together, our results indicated that GLP-1R is of vital importance for memory maintenance and neuronal mitophagy, and baicalein markedly improved cognitive impairment in diabetes through enhancing mitophagy. This work strengthened the notion that GLP-1R is required for the mitophagy recovery of neurons, and the proposed mechanisms of baicalein to alleviate cognitive disorder of diabetes have been summarized in Fig. 10.

In conclusion, baicalein is a potential GLP-1R small-molecule agonist, which has beneficial effects on improving cognitive function of diabetic mice. The underlying mechanisms might involve increasing mitophagy levels via GLP-1R. The study provides new insight into the development of GLP-1R agonists and potential new drugs to treat diabetic cognitive disorder.

CRediT author statement

Na Liu: Data curation, Methodology, Formal analysis, Validation, Project administration, Writing - Original draft preparation; **Xin Cui**, **Wenhui Yan** and **Tingli Guo**: Methodology, Validation; **Zhuanzhuan Wang**: Investigation, Methodology; **Xiaotong Wei**, **Yuzhuo Sun** and **Jieyun Liu**: software; **Cheng Xian**: Validation, Supervision; **Weina Ma** and **Lina Chen**: Funding acquisition, Project administration, Writing - Reviewing and Editing.

Declaration of competing interest

The authors declare that the Editor-in-Chief Prof. Langchong He and the Section Editor Weina Ma didn't give additional favor for the submittion and publication of this work. And we declare that no known competing financial interests or personal relationships could have appeared to influence the work.

Acknowledgments

This work was funded by the Fundamental Research Funds for the Central Universities (Grant No.: xzd012022099), Natural Science Basic Research Program of Shaanxi (Grant Nos.: 2023-JC-ZD-47, and 2023-JC-QN-0921), Research Project of Shaanxi Administration of Traditional Chinese Medicine (Project No.: SZY-KJCYC-2023-008), Research Project of Guangxi Administration of Traditional Chinese Medicine (Project No.: GXZYJ20230711), and Basic & Clinical Sciences Integration Innovation Project of Xi'an Jiaotong University (Project No.: YXJLRH2022018).

The authors thank the efforts of all the members from NLERC of Screening & Analysis for Natural Vascular Medicine Lab of Xian Jiaotong University and Biomedical Experimental Center of Xi'an Jiaotong University. Especially, Langchong He for his effort on experiment platform bulit, Shengli Han and Nan Wang for their advices and technical assistance. We also thank Hao Hu for his contribution on MWM test.

Appendix A. Supplementary data

Supplementary data to this article can be found online at https://doi.org/10.1016/j.jpha.2024.100968.

References

[1] A. Artasensi, A. Pedretti, G. Vistoli, et al., Type 2 diabetes mellitus: A review of multi-target drugs, Molecules 25 (2020), 1978.
[2] G.J. Biessels, F. Despa, Cognitive decline and dementia in diabetes mellitus: Mechanisms and clinical implications, Nat. Rev. Endocrinol. 14 (2018) 591–604.
[3] R.J. McCrimmon, C.M. Ryan, B.M. Frier, Diabetes and cognitive dysfunction, Lancet 379 (2012) 2291–2299.
[4] G. Ashrafi, T.L. Schwarz, The pathways of mitophagy for quality control and clearance of mitochondria, Cell Death Differ. 20 (2013) 31–42.
[5] S. Pickles, P. Vigié, R.J. Youle, Mitophagy and quality control mechanisms in mitochondrial maintenance, Curr. Biol. 28 (2018) R170–R185.
[6] X. Ge, L. Wang, Q. Cui, et al., Electroacupuncture improves cognitive impairment in diabetic cognitive dysfunction rats by regulating the mitochondrial autophagy pathway, J. Physiol. Sci. 72 (2022), 29.
[7] Y. Song, Y. Du, W. Zou, et al., Involvement of impaired autophagy and mitophagy in Neuro-2a cell damage under hypoxic and/or high-glucose conditions, Sci. Rep. 8 (2018), 3301.
[8] Z. Wang, P. Xia, J. Hu, et al., LncRNA MEG3 alleviates diabetic cognitive impairments by reducing mitochondrial-derived apoptosis through promotion of FUNDC1-related mitophagy via Rac1-ROS axis, ACS Chem. Neurosci. 12 (2021) 2280–2307.
[9] Y. Zhou, L. Huang, W. Zheng, et al., Recurrent nonsevere hypoglycemia exacerbates imbalance of mitochondrial homeostasis leading to synapse injury and cognitive deficit in diabetes, Am. J. Physiol. Endocrinol. Metab. 315 (2018) E973–E986.
[10] J. Lv, S. Jiang, Z. Yang, et al., PGC-1α Sparks the fire of neuroprotection against neurodegenerative disorders, Ageing Res. Rev. 44 (2018) 8–21.
[11] N.M.B. Yapa, V. Lisnyak, B. Reljic, et al., Mitochondrial dynamics in health and disease, FEBS Lett. 595 (2021) 1184–1204.
[12] K. Palikaras, E. Lionaki, N. Tavernarakis, Coordination of mitophagy and mitochondrial biogenesis during ageing in C. elegans, Nature 521 (2015) 525–528.
[13] H. Cai, D. Yang, J. Qiao, et al., A GLP-1/GIP dual receptor agonist DA4-JC effectively attenuates cognitive impairment and pathology in the APP/PS1/tau model of Alzheimer's disease, J. Alzheimers. Dis. 83 (2021) 799–818.
[14] A.J.M. Chaves Filho, N.L. Cunha, A.G. de Souza, et al., The GLP-1 receptor agonist liraglutide reverses *Mania*-like alterations and memory deficits induced by D-amphetamine and augments lithium effects in mice: Relevance for bipolar disorder, Prog. Neuropsychopharmacol Biol. Psychiatry 99 (2020), 109872.
[15] H. Zhang, Y. Chu, H. Zheng, et al., Liraglutide improved the cognitive function of diabetic mice via the receptor of advanced glycation end products down-regulation, Aging 13 (2020) 525–536.
[16] H. Yi, Y. Duan, R. Song, et al., Activation of glucagon-like peptide-1 receptor in microglia exerts protective effects against sepsis-induced encephalopathy via attenuating endoplasmic reticulum stress-associated inflammation and apoptosis in a mouse model of sepsis, Exp. Neurol. 363 (2023), 114348.
[17] T. Kawai, B. Sun, H. Yoshino, et al., Structural basis for GLP-1 receptor activation by LY3502970, an orally active nonpeptide agonist, Proc. Natl. Acad. Sci. U. S. A. 117 (2020) 29959–29967.
[18] M. Davies, T.R. Pieber, M.L. Hartoft-Nielsen, et al., Effect of oral semaglutide compared with placebo and subcutaneous semaglutide on glycemic control in patients with type 2 diabetes: A randomized clinical trial, JAMA 318 (2017) 1460–1470.
[19] F.S. Willard, J.D. Ho, K.W. Sloop, Discovery and pharmacology of the covalent GLP-1 receptor (GLP-1R) allosteric modulator BETP: A novel tool to probe GLP-1R pharmacology, Adv. Pharmacol. 88 (2020) 173–191.
[20] A. Thompson, J.W. Stephens, S.C. Bain, et al., Molecular characterisation of small molecule agonists effect on the human glucagon like peptide-1 receptor internalisation, PLoS One 11 (2016), e0154229.
[21] W. Ma, C. Wang, R. Liu, et al., Advances in cell membrane chromatography, J. Chromatogr. A 1639 (2021), 461916.
[22] T. Zhao, H. Tang, L. Xie, et al., *Scutellaria baicalensis* Georgi. (Lamiaceae): A review of its traditional uses, botany, phytochemistry, pharmacology and toxicology, J. Pharm. Pharmacol. 71 (2019) 1353–1369.
[23] Y. Wang, Z. Liu, G. Liu, et al., Research progress of active ingredients of *Scutellaria baicalensis* in the treatment of type 2 diabetes and its complications, Biomed. Pharmacother. 148 (2022), 112690.
[24] A. Ahmadi, Z. Mortazavi, S. Mehri, et al., *Scutellaria baicalensis* and its constituents baicalin and baicalein as antidotes or protective agents against chemical toxicities: A comprehensive review, Naunyn Schmiedebergs Arch. Pharmacol. 395 (2022) 1297–1329.
[25] L. Duan, Y. Zhang, Y. Yang, et al., Baicalin inhibits ferroptosis in intracerebral hemorrhage, Front. Pharmacol. 12 (2021), 629379.
[26] Y. Lv, S. Wang, P. Liang, et al., Screening and evaluation of anti-SARS-CoV-2 components from *Ephedra sinica* by ACE2/CMC-HPLC-IT-TOF-MS approach, Anal. Bioanal. Chem. 413 (2021) 2995–3004.
[27] W. Ma, L. Yang, Y. Lv, et al., Determine equilibrium dissociation constant of drug-membrane receptor affinity using the cell membrane chromatography relative standard method, J. Chromatogr. A 1503 (2017) 12–20.
[28] X. He, Y. Sui, S. Wang, Application of a stepwise frontal analysis method in cell membrane chromatography, J. Chromatogr. B Analyt. Technol. Biomed. Life Sci. 1161 (2020), 122436.
[29] R. Moaddel, I.W. Wainer, Development of immobilized membrane-based affinity columns for use in the online characterization of membrane bound proteins and for targeted affinity isolations, Anal. Chim. Acta 564 (2006) 97–105.
[30] Q. Jia, J. Fu, C. Gao, et al., MrgX2-SNAP-tag/cell membrane chromatography model coupled with liquid chromatography-mass spectrometry for anti-pseudo-allergic compound screening in Arnebiae Radix, Anal. Bioanal. Chem. 414 (2022) 5741–5753.
[31] X. Yi, W. Yan, T. Guo, et al., Erythropoietin mitigates diabetic nephropathy by restoring PINK1/parkin-mediated mitophagy, Front. Pharmacol. 13 (2022), 883057.
[32] W. Tang, Y. Li, S. He, et al., *Caveolin-1* alleviates diabetes-associated cognitive dysfunction through modulating neuronal ferroptosis-mediated mitochondrial homeostasis, Antioxid. Redox Signal. 37 (2022) 867–886.
[33] W.M. Nolte, J.P. Fortin, B.D. Stevens, et al., A potentiator of orthosteric ligand activity at GLP-1R acts via covalent modification, Nat. Chem. Biol. 10 (2014) 629–631.
[34] L.B. Bergantin, Diabetes and inflammatory diseases: An overview from the perspective of Ca^{2+}/3'-5'-cyclic adenosine monophosphate signaling, World J. Diabetes 12 (2021) 767–779.
[35] X.-F. Zhao, G protein-coupled receptors function as cell membrane receptors for the steroid hormone 20-hydroxyecdysone, Cell Commun. Signal. 18 (2020), 146.
[36] J. Damanik, E. Yunir, Type 2 diabetes mellitus and cognitive impairment, Acta Med. Indones. 53 (2021) 213–220.
[37] B. Dinda, S. Dinda, S. DasSharma, et al., Therapeutic potentials of baicalin and its aglycone, baicalein against inflammatory disorders, Eur. J. Med. Chem. 131 (2017) 68–80.
[38] J. Zhu, C. Chen, B. Zhang, et al., The inhibitory effects of flavonoids on α-amylase and α-glucosidase, Crit. Rev. Food Sci. Nutr. 60 (2020) 695–708.

[39] S. Sajadimajd, N. Deravi, K. Forouhar, et al., Endoplasmic reticulum as a therapeutic target in type 2 diabetes: Role of phytochemicals, Int. Immunopharmacol. 114 (2023), 109508.
[40] B.-W. Zhang, X. Li, W.-L. Sun, et al., Dietary flavonoids and acarbose synergistically inhibit α-glucosidase and lower postprandial blood glucose, J. Agric. Food Chem. 65 (2017) 8319−8330.
[41] S. Gupta, H.S. Buttar, G. Kaur, et al., Baicalein: Promising therapeutic applications with special reference to published patents, Pharm. Pat. Anal. 11 (2022) 23−32.
[42] H. Xue, Y. Huo, Y. Hu, et al., The role of ALOX15B in heat stress-induced apoptosis of porcine sertoli cells, Theriogenology 185 (2022) 6−15.
[43] Y. Li, X. Zheng, X. Yi, et al., Myricetin: A potent approach for the treatment of type 2 diabetes as a natural class B GPCR agonist, FASEB J. 31 (2017) 2603−2611.
[44] G. Gupta, M.A. Siddiqui, M.M. Khan, et al., Current pharmacological trends on myricetin, Drug Res. (Stuttg) 70 (2020) 448−454.
[45] R. Dhanya, Quercetin for managing type 2 diabetes and its complications, an insight into multitarget therapy, Biomed. Pharmacother. 146 (2022), 112560.
[46] Z. Wang, M. Zeng, Z. Wang, et al., Dietary luteolin: A narrative review focusing on its pharmacokinetic properties and effects on glycolipid metabolism, J. Agric. Food Chem. 69 (2021) 1441−1454.
[47] A. Caselli, P. Cirri, A. Santi, et al., Morin: A promising natural drug, Curr. Med. Chem. 23 (2016) 774−791.
[48] L. Yao, W. Liu, M. Bashir, et al., Eriocitrin: A review of pharmacological effects, Biomed. Pharmacother. 154 (2022), 113563.
[49] Z. Cong, L.-N. Chen, H. Ma, et al., Molecular insights into ago-allosteric modulation of the human glucagon-like peptide-1 receptor, Nat. Commun. 12 (2021), 3763.
[50] G. Song, D. Yang, Y. Wang, et al., Human GLP-1 receptor transmembrane domain structure in complex with allosteric modulators, Nature 546 (2017) 312−315.
[51] L.-H. Zhao, Y. Yin, D. Yang, et al., Differential requirement of the extracellular domain in activation of class B G protein-coupled receptors, J. Biol. Chem. 291 (2016) 15119−15130.
[52] G.D. Stanciu, V. Bild, D.C. Ababei, et al., Link between diabetes and Alzheimer's disease due to the shared amyloid aggregation and deposition involving both neurodegenerative changes and neurovascular damages, J. Clin. Med. 9 (2020), 1713.
[53] S.T. Ferreira, Brain insulin, insulin-like growth factor 1 and glucagon-like peptide 1 signalling in Alzheimer's disease, J. Neuroendocrinol. 33 (2021), e12959.
[54] R. Ravona-Springer, E. Moshier, J. Schmeidler, et al., Changes in glycemic control are associated with changes in cognition in non-diabetic elderly, J. Alzheimers. Dis. 30 (2012) 299−309.
[55] I. Feinkohl, J.F. Price, M.W. Strachan, et al., The impact of diabetes on cognitive decline: Potential vascular, metabolic, and psychosocial risk factors, Alzheimers. Res. Ther. 7 (2015), 46.
[56] Y. Zhang, W. Song, Islet amyloid polypeptide: Another key molecule in Alzheimer's pathogenesis? Prog. Neurobiol. 153 (2017) 100−120.
[57] D.J. Drucker, Mechanisms of action and therapeutic application of glucagon-like peptide-1, Cell Metab. 27 (2018) 740−756.
[58] C.S. Bae, J. Song, The role of glucagon-like peptide 1 (GLP1) in type 3 diabetes: GLP-1 controls insulin resistance, neuroinflammation and neurogenesis in the brain, Int. J. Mol. Sci. 18 (2017), 2493.
[59] S.M. Day, W. Yang, X. Wang, et al., Glucagon-like peptide-1 cleavage product improves cognitive function in a mouse model of down syndrome, eNeuro 6 (2019) ENEURO.0031-ENEURO.0019.2019.
[60] A.F. Batista, L. Forny-Germano, J.R. Clarke, et al., The diabetes drug liraglutide reverses cognitive impairment in mice and attenuates insulin receptor and synaptic pathology in a non-human primate model of Alzheimer's disease, J. Pathol. 245 (2018) 85−100.
[61] M.S. Mohiuddin, T. Himeno, R. Inoue, et al., Glucagon-like peptide-1 receptor agonist protects dorsal root ganglion neurons against oxidative insult, J. Diabetes Res. 2019 (2019), 9426014.
[62] A. Khalilnezhad, D. Taskiran, The investigation of protective effects of glucagon-like peptide-1 (GLP-1) analogue exenatide against glucose and fructose-induced neurotoxicity, Int. J. Neurosci. 129 (2019) 481−491.
[63] A.I. Duarte, E. Candeias, I.N. Alves, et al., Liraglutide protects against brain amyloid-β_{1-42} accumulation in female mice with early Alzheimer's disease-like pathology by partially rescuing oxidative/nitrosative stress and inflammation, Int. J. Mol. Sci. 21 (2020), 1746.
[64] S. Lefort, M.H. Tschöp, C. García-Cáceres, A synaptic basis for GLP-1 action in the brain, Neuron 96 (2017) 713−715.
[65] J.G. Barrera, K.R. Jones, J.P. Herman, et al., Hyperphagia and increased fat accumulation in two models of chronic CNS glucagon-like peptide-1 loss of function, J. Neurosci. 31 (2011) 3904−3913.
[66] M. Haddadi, S.R. Jahromi, B.K. Chandrasekhar Sagar, et al., Brain aging, memory impairment and oxidative stress: A study in Drosophila melanogaster, Behav. Brain Res. 259 (2014) 60−69.
[67] L.-Q. Zhang, W. Zhang, T. Li, et al., GLP-1R activation ameliorated novel-object recognition memory dysfunction via regulating hippocampal AMPK/NF-κB pathway in neuropathic pain mice, Neurobiol. Learn. Mem. 182 (2021), 107463.
[68] W. Bakker, M. Imbernon, C.G. Salinas, et al., Acute changes in systemic glycemia gate access and action of GLP-1R agonist on brain structures controlling energy homeostasis, Cell Rep. 41 (2022), 111698.
[69] H. Zhang, B. Song, W. Zhu, et al., Glucagon-like peptide-1 attenuated carboxymethyl lysine induced neuronal apoptosis via peroxisome proliferation activated receptor-γ, Aging (Albany NY) 13 (2021) 19013−19027.
[70] T. Wai, T. Langer, Mitochondrial dynamics and metabolic regulation, Trends Endocrinol. Metab. 27 (2016) 105−117.
[71] M.C. Hsu, B.C. Guo, C.H. Chen, et al., Apigenin ameliorates hepatic lipid accumulation by activating the autophagy-mitochondria pathway, J. Food Drug Anal. 29 (2021) 240−254.
[72] T. Eisenberg, M. Abdellatif, S. Schroeder, et al., Cardioprotection and lifespan extension by the natural polyamine spermidine, Nat. Med. 22 (2016) 1428−1438.
[73] A.K. Torres, C. Jara, H.S. Park-Kang, et al., Synaptic mitochondria: An early target of amyloid-β and tau in Alzheimer's disease, J. Alzheimers. Dis. 84 (2021) 1391−1414.
[74] J.S. Kerr, B.A. Adriaanse, N.H. Greig, et al., Mitophagy and Alzheimer's disease: Cellular and molecular mechanisms, Trends Neurosci. 40 (2017) 151−166.
[75] D. Trigo, C. Avelar, M. Fernandes, et al., Mitochondria, energy, and metabolism in neuronal health and disease, FEBS Lett. 596 (2022) 1095−1110.
[76] F. Yang, X. Wang, J. Qi, et al., Glucagon-like peptide 1 receptor activation inhibits microglial pyroptosis via promoting mitophagy to alleviate depression-like behaviors in diabetic mice, Nutrients 15 (2022), 38.